Global Environmental Science
www.sciltp.com/journals/ges

Review

Catalytic Elimination of Typical Halogenated Volatile Organic Compounds (HVOCs): A Critical Review

Qinpei Sun [1], Xiaohui Yu [2], Keying Shang [1], Linke Wu [1], Peiqi Chu [1], Yuxi Liu [1,3], Jiguang Deng [1,3], Zhiquan Hou [1,3] and Hongxing Dai [1,3,*]

[1] Beijing Key Laboratory for Green Catalysis and Separation, State Key Laboratory of Materials Low-Carbon Recycling, Laboratory of Catalysis Chemistry and Nanoscience, Department of Chemical Engineering and Technology, College of Materials Science and Engineering, Beijing University of Technology, Beijing 100124, China
[2] Salt Lake Chemical Engineering Research Complex, School of Chemical Engineering, Qinghai University, Xining 810016, China
[3] Key Laboratory of Beijing on Regional Air Pollution Control, College of Environmental Science and Engineering, Beijing University of Technology, Beijing 100124, China
* Correspondence: hxdai@bjut.edu.cn

How To Cite: Sun, Q.; Yu, X.; Sang, K.; et al. Catalytic Elimination of Typical Halogenated Volatile Organic Compounds (HVOCs): A Critical Review. *Glob. Environ. Sci.* **2025**, *1*(2), 134–156. https://doi.org/10.53941/ges.2025.100012

Publication History

Received: 14 October 2025
Revised: 6 November 2025
Accepted: 14 November 2025
Published: 20 November 2025

Keywords

halogenated volatile organic compound; catalytic elimination; catalyst preparation method; catalytic reaction mechanism; catalyst deactivation

Highlights

- Preparation methods of the catalysts for halogenated volatile organic compounds elimination are summarized.
- Catalytic elimination of halogenated volatile organic compounds is reviewed.
- Catalytic removal mechanisms of halogenated volatile organic compounds are discussed.
- Prospects and challenges of catalytic halogenated volatile organic compounds elimination are proposed.

Abstract: Halogenated volatile organic compounds (HVOCs) represent a class of highly toxic, stable, and recalcitrant organic compounds among the volatile organic compounds (VOCs), posing big threats to air quality and human health. Catalytic elimination is a promising approach for HVOCs purification. However, catalytic elimination of HVOCs generates highly reactive and corrosive HX and X_2 (X = F, Cl, and Br), giving rise to the poisoning and deactivation of catalysts. Moreover, the formation of numerous halogen-containing byproducts can induce secondary pollution issues. Therefore, the development of catalysts with high stability, good catalytic performance, and low selectivity towards toxic byproducts has been the primary research focus in the past years. Modifying geometric and electronic structures of the catalysts and constructing bifunctional catalysts with synergistic acidity and redox properties have demonstrated good catalytic performance and resistance towards poisoning. Depending on the category of HVOCs, different catalytic reaction systems are often required. The present review article summarizes recent progresses in catalysts preparation and their catalytic HVOCs elimination performance. By categorizing HVOCs removal into several specific reaction systems, we discuss the deep elimination efficiency of HVOCs, the selectivity of inorganic halogen species, and the migration pathways and removal mechanisms of halogens on the catalysts surface, thereby establishing the structure–performance relationships. Furthermore, we outline the prospects and challenges of catalytic HVOCs elimination technologies in the future work and practical applications. It is expected that the findings summarized in this review will inspire more researchers to develop catalytic systems capable of effectively eliminating HVOCs.

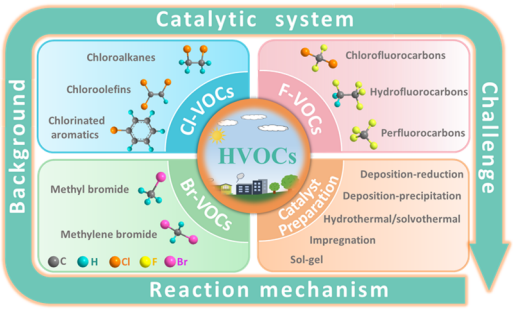

1. Introduction

Halogenated volatile organic compounds (HVOCs) are a class of organic substances which are particularly challenging to manage among volatile organic compounds (VOCs), including fluorinated, chlorinated, and brominated volatile organic compounds (F-VOCs, Cl-VOCs, and Br-VOCs), respectively. Compared to traditional VOCs, HVOCs are featured by strong toxicity, high stability, difficulty in degradation, and a strong potential to deplete the ozone layer, thus leading to strict regulatory controls [1]. Cl-VOCs primarily originate from the chloro-alkali chemical industry (e.g., ethyl chloride) and the fine chemical/pharmaceutical industry (e.g., dichloromethane), with incineration and catalytic oxidation processes in the presence of Cl-VOCs generating significant amounts of dioxins [2]. F-VOCs are typical ozone-depleting substances and potent greenhouse gases. Chlorofluorocarbons (CFCs) and hydrofluorocarbons (HFCs) are widely used as blowing agents and refrigerants due to their stable molecular structures and good thermodynamic properties. The Montreal Protocol on Substances that Deplete the Ozone Layer has imposed strict regulations on the production of CFCs and halons. The primary emission sources of the strong greenhouse gas CF_4 (Global warming potential (GWP) = 6500) are the aluminum electrolysis and semiconductor industries [3–5]. Global warming has become one of the most pressing issues in the 21st century. Current global emissions of F-containing gases exceed 1 billion tons of CO_2 equivalents annually [6]. The Kyoto Protocol and the Carbon Border Adjustment Mechanism issued by European Union have identified HFCs and PFCs as key greenhouse gases, respectively. In addition, Br-VOCs, with their strong ozone-depleting potential, are extensively used and emitted in industries such as fumigation and purified terephthalic acid (PTA), causing persistent and irreversible damage to the atmosphere environment [7–9]. Due to the persistent damage caused by persistent organic pollutants (POPs) and their resistance to degradation, the Stockholm Convention on POPs strictly limits their emissions [10]. More severely, the complete substitution or elimination of HVOCs in the source of these industries is not feasible in the short term. Therefore, end-of-pipe treatment methods for purifying exhaust gases containing HVOCs remain essential, with catalytic removal being one of the most effective methods for HVOCs removal [11–13].

The significant electronegativity difference between fluorine and carbon in F-VOCs results in the strong C–F bond energies. In the catalytic elimination of CX_4 (X = halogen)-type compounds, the fundamental reaction is hydrolysis. Previous studies have suggested that the hydrolysis of CX_4 to CO_2 does not require oxygen. However, the complete decomposition of C_2 compounds, HFCs, and CFCs necessitates the involvement of oxygen in addition to water [14]. Catalytic combustion and catalytic hydrolysis can completely mineralize them into CO_2 and HF. Research has been primarily focused on solid acid catalysts [15–18], but excessive acidity would lead to carbon deposition. Fluorination can cause irreversible catalyst deactivation. Conventional halogen poisoning of catalysts occurs when halogen–carbon bonds are dissociated from HVOCs molecules and the generated halogen atoms are strongly adsorbed on the active metal centers, leading to gradual deactivation. Traditional strategies to combat deactivation involve reducing the binding strength between halogen and metal center to facilitate rapid dehalogenation [2,19]. In the catalytic elimination of F-VOCs, however, the highly reactive fluorine species generated may undergo fluorination, involving the substitution of lattice oxygen on the catalyst surface by fluorine atoms, which can destroy the catalyst crystal structures and affect their long-term stability [18]. Introducing water as a new proton donor promotes the migration of fluorine species on the catalyst surface, inhibits fluorine poisoning, and may enhance C–F bond activation compared to the original hydroxyl groups in the catalysts [5]. Current research lacks exploration of the migration pathways of fluorine species on the catalyst surface and attention to complex industrial exhaust gases (e.g., containing SO_2 and multi-component mixed F-VOCs). The products of catalytic Cl-VOCs oxidation are highly complex, with H_2O, CO_2, and HCl being the desired final products [19–24]. The migration and transformation ways of Cl species include HCl desorption from the Brønsted acid sites, Cl_2 generation via the Deacon reaction, organic byproducts from the chlorination reactions, and Cl deposition on the catalyst surface. Promoting deep oxidation reactions and inhibiting chlorination reactions are primary strategies for controlling byproduct formation. Introducing Brønsted acid sites can effectively facilitate HCl desorption. Rational regulation of redox properties of catalysts enables deep oxidation of intermediates at low temperatures. Designing the catalysts with closely coupled acidic and redox sites can enhance catalytic performance and decrease the selectivities towards toxic byproducts. The introduction of water can remove surface byproducts but may also compete with reactants for adsorption at the active sites, hence generating more non-chlorinated byproducts. The positive or negative effect of water on catalytic Cl-VOCs elimination depends mainly upon its concentration and reaction temperature [2]. Catalytic elimination of the Br-VOCs (e.g., CH_3Br) faces similar challenges to that of the Cl-VOCs, including catalyst deactivation by HBr or Br_2 poisoning and high selectivities towards the polybrominated byproducts [25–27]. However, there are distinct differences between catalytic combustion of the Br-VOCs and the chlorinated and fluorinated hydrocarbons. For instance, the latter two can increase the selectivities towards hydrogen halides by

adding water and hydrogen (hydrocarbons) as hydrogen sources, thereby reducing their poisoning effects on the catalyst. In contrast, elemental bromine may exhibit a high selectivity during catalytic brominated alkanes combustion processes. High selectivity to Br_2 can give rise to rapid catalyst deactivation and formation of the polybrominated byproducts. Current catalyst development for Br-VOCs elimination is often tailored for specific industries, in which there are more complex exhaust gas compositions under actual operating conditions. These characteristics pose new questions and challenges in developing the catalysts for the elimination of brominated hydrocarbons.

Traditional catalytic oxidation typically refers to the chemical process of completely converting organic pollutants into CO_2, H_2O, and other harmless small molecules (such as N_2, HCl, etc.) in the presence of a catalyst and oxygen at certain temperatures [2,19]. Catalytic oxidation can achieve the VOCs removal efficiency up to 99%, and the presence of a catalyst significantly lowers the ignition temperature of the reaction (usually between 200 and 500 °C), thus greatly reducing fuel consumption and operating cost. However, the cost of the noble metal catalysts is high. In addition, certain substances in the exhaust gases can cause permanent or temporary deactivation of the catalysts for the elimination of HVOCs, and insufficient catalyst lifespan and activity may necessitate frequent replacements, which represents the biggest challenge faced by the traditional catalytic oxidation [1]. Therefore, to achieve efficient catalytic elimination of HVOCs, it is often necessary to develop more suitable catalytic elimination methods based on actual operating conditions (such as catalytic hydrolysis, synergistic photothermocatalysis, etc.) [5,28,29]. This review aims to systematically summarize the latest research advancements and future challenges in catalyst preparation methods and catalytic HVOCs elimination performance. We categorize the HVOCs based on their molecular structural characteristics and focus on catalytic systems, design strategies for catalytic materials, catalytic performance and structure–activity relationships, and catalytic reaction/deactivation mechanisms for the removal of Cl-, F-, and Br-VOCs. Particular emphasis is placed on the catalytic elimination systems for typical greenhouse gases and emerging pollutants. Current research primarily focuses on typical pollutants (e.g., Cl-VOCs), with fewer comprehensive reviews being dedicated to the HVOCs treatment. In addition, we still hope that this review article can also provide an outlook for future research directions to offer a theoretical guidance for the development of highly efficient catalysts. Table 1 provides a list of abbreviations used in this review article.

Table 1. List of abbreviations.

Name	Abbreviation	Name	Abbreviation
volatile organic compounds	VOCs	trichlorofluoromethane	CFC-13
halogenated volatile organic compounds	HVOCs	dibromomethane	DBM
fluorinated volatile organic compounds	F-VOCs	dioxymethylene	DOM
chlorinated volatile organic compounds	Cl-VOCs	methyl bromide	MB
brominated volatile organic compounds	Br-VOCs	chlorobenzene	CB
persistent organic pollutants	POPs	dichloromethane	DCM
purified terephthalic acid	PTA	1,2-dichloroethane	1,2-DCE
global warming potential	GWP	vinyl chloride	VC
deposition-reduction	DR	p-xylene	PX
deposition-precipitation	DP	trichloroethylene	TCE
Metal-organic frameworks	MOFs	tetrachloroethylene	PCE
dry impregnation	DI	density functional theory	DFT
wet impregnation	WI	space velocity	SV
chlorofluorocarbons	CFCs	3-coordinated Al	$1Al_{3c}$
hydrofluorocarbons	HFCs	protonated sulfate	$-HSO_4$
perfluorocarbons	PFCs	Mars–van Krevelen	MvK
1,1,1,2-Tetrafluoroethane	HFC-134a	Hard–Soft–Acid–Base	HSAB
dichlorodifluoromethane	CFC-12		

2. Catalyst Types and Preparation

Catalysts are the cornerstone of catalytic elimination technology. The rational designing of catalytic systems with high performance and good stability is crucial for improving the catalytic elimination efficiency of HVOCs [30–32]. Supported noble metals [33–41], transition metal oxides [42,43], composite metal oxides [44,45] and Zeolite-based catalysts [23,46] are the most commonly used catalysts. Noble metals are highly favored for the catalytic elimination of HVOCs. The loading of noble metals can improve the interactions with the supports, and the catalytic performance is governed by particle size, shape, and loading amount of the noble metal(s). Among the platinum group metals, Ru is the most cost-effective and exhibits the highest catalytic activity. Ru demonstrates the highest chlorine removal ability and the lowest yield of polychlorinated byproducts [20,21].

 https://doi.org/10.53941/ges.2025.100012

Additionally, Pt is another research hotspot among the noble metal catalysts. Owing to its excellent redox property, Pt can promote the deep oxidation of halogenated pollutants to CO_2, while reducing carbon deposition on the catalyst surface and enhancing its stability [33]. However, the activity of noble metals may be constrained by the nature of the support and the target pollutants. Transition metal oxides represent another class of catalyst materials for the elimination of HVOCs. Compared to noble metals, transition metal oxides are widely used due to their low cost and good redox properties, but these materials are more susceptible to the formation of byproducts. It is important that the preparation method of a catalyst determines chemical state of the active component(s) on its surface. Appropriate preparation approaches help to better achieve surface functionalization and can regulate the electronic structure and defect sites of catalysts.

2.1. Supported Noble Metals Catalysts

The dispersion of small amounts of noble metals on various metal oxide supports can increase redox ability and acidity of the catalysts. The unfilled outer d-electron orbitals of noble metals facilitate adsorption and activation of the reactants during the elimination of HVOCs. Supported noble metal catalysts exhibit good low-temperature catalytic activities and minimal formation of the halogenated byproducts. Maupin et al. [33] studied the dichloromethane (DCM) oxidation mechanisms over Pt/γ-Al_2O_3 under humid conditions. They claimed that the oxidation of DCM initially formed incomplete oxidation products (e.g., carbon monoxide and chloromethane) on the support, which were then further oxidized to hydrogen chloride and carbon dioxide that was facilitated by the redox property of platinum. However, noble metals are inherently expensive, easy sintering at high temperatures, and susceptible to deactivation by halogen deposition. Different preparation methods can significantly alter the particle sizes and dispersion of noble metals on the surface of the support, hence influencing the strong interaction between metal and support.

The impregnation strategy is one of the most straightforward methods for preparing supported catalysts in industrial applications, and its fundamental principle involves utilizing capillary forces to adsorb metal precursors into the porous supports. Using a precursor solution that exceeds the pore volume of the support results in a slurry, which is known as the wet impregnation (WI) method. Limiting the solution volume to just fill the pore volume of a support is termed the dry impregnation (DI) method [34]. In the WI method, the impregnated support is filtered, leaving behind the excessive liquid containing unretained precursors. This necessitates the recovery of the excess liquid to minimize precursor waste. The use of the DI method eliminates the need for filtration by removing the excess liquid. However, the absence of a filtration step in the DI method means that the counterions from the metal precursor salts, such as chloride from ruthenium chloride ($RuCl_3$), will be remained in the dried catalyst. To obtain the final catalysts with stable metal particles on the support, the impregnated and dried powders are calcined in the oxidizing and/or reducing atmospheres for the removal of the precursor ligands. The primary disadvantage of the traditional impregnation method is the poor dispersion of metal particles and the difficulty in controlling particle sizes due to the lack of inducing interactions between metal precursors and support. For instance, during the drying process, the concentration of the metal precursor solution may reach supersaturation, leading to precipitation and ultimately reducing distribution of the active phase. The pH of the support-impregnating solution paste is likely to reach the point of zero charge of the support by the abundant surface hydroxyl groups, which far exceeds the solution acid or base content that can protonate or deprotonate the surface [34]. The sizes and dispersion of noble metals can be precisely controlled by adjusting the impregnation parameters, adding organic molecules to alter the interaction between the salt solution and the support, and coordinating with the metal [35,36]. For the supported catalysts, the property of a support is also a significant factor influencing catalytic performance. Differences in type, preparation method, and crystal structure of the support can affect the interaction between the support and the active sites [2]. For example, Liu et al. [37] investigated the catalytic oxidation activity of TCE over the Ru catalysts supported on titanium dioxide with three different crystal phases, and found that the active component RuO_x in the Ru catalysts supported on titanium dioxide with three different crystal phases exhibited different catalytic behaviors. RuO_x was highly unstable on the anatase TiO_2 and tended to sinter, while the rutile TiO_2 allowed RuO_x to better retain its original form.

The deposition-reduction (DR) method involves three core steps, i.e., liquid-phase reduction, adsorption deposition, and immobilization. Liquid-phase reduction is one of the simplest methods for preparing noble metal nanoparticles, since noble metal nanoparticles can be directly obtained from various precursor compounds dissolved in specific solvents [34]. Initially, noble metal precursors are dissolved in a suitable solvent to form a homogeneous solution. Subsequently, reducing agents and stabilizers are added [20,21]. Under mild conditions, noble metal ions are reduced to zero-valent metal atoms. These newly generated metal atoms aggregate to form nuclei and continue to grow into nanoparticles. The stabilizer are adsorbed on the surface of noble metal nanoparticles through steric hindrance or electrostatic repulsion to prevent excessive growth and aggregation of

noble metal nanoparticles, hence forming a uniform and stable colloidal solution. The newly generated noble metal nanoparticles are then loaded on the support surface. The sizes and structures of noble metal nanoparticles can be accurately controlled by adjusting the solution parameters, thus allowing for the pre-synthesis of highly uniform and specific nanoparticles. Compared to the traditional impregnation methods, this approach possesses significant advantages in controlling particle dispersion and reducing metal aggregation. However, the DR method also faces several challenges: (i) Weak interaction between metal and support: Metal nanoparticles are encapsulated by stabilizers, and the direct contact and chemical bonding between the "pre-formed" particles and the support may be weak. (ii) Stabilizer removal dilemma: To expose the active sites, the conditions for removing the stabilizer covering the metal particles must be strictly controlled; otherwise, it can easily lead to the aggregation and growth of metal nanoparticles, thereby reducing metal particle dispersion and catalytic activity. (iii) Loading limit: Nanoparticles are likely to aggregate at high loadings, making uniform dispersion difficult to be achieved. Future development of the DR method will be focused on selecting the new environmentally friendly stabilizers and enhancing the interaction between metal nanoparticles and support (e.g., by introducing oxygen vacancies and functional groups to modify the support).

The deposition-precipitation (DP) method is also commonly employed for fabricating the supported metal catalysts. Metal salt precursors form low-solubility metal hydroxides under the influence of precipitants or complexing agents [35]. To guarantee that precipitation occurs exclusively on the support surface and does not take place in the solution, two main conditions must be satisfied: (i) A strong interaction between dissolved metal (M) precursor and support; and (ii) control of the precursor concentration in the solution to prevent spontaneous precipitation. When the support combines with the metal hydroxide complex to form the M–O–support bonds, a state of uniform distribution and concentrated active material is achieved. For the uniform precipitation to occur, the nucleation rate on the support must be higher than that in the bulk solution, while maintaining homogeneity of the solution. For instance, urea can act as a mild base, which precipitates the metals on the support as the temperature rises during the DP process [38]. Lysine complexes with the metal ions to prevent metal phase aggregation during the DP process [39]. The advantage of the DP method is its independence from solubility, with the metal loadings on the support far exceeding those achievable by the impregnation method. Due to the poor control in metal distribution and surface composition, however, it is full of challenge to prepare bimetallic catalysts with controllable compositions.

In addition to the aforementioned conventional methods, researchers have developed various more advanced approaches for preparing supported noble metal catalysts. For instance, Simon et al. [40] fabricated the Pt-CeO_2 porous thin films on the Si substrate via a direct liquid injection-chemical vapor deposition route. Pt diffused through and decomposed within the porous structure of the pre-formed CeO_2 thin film. When the Pt^{2+} sites on CeO_2 reached a saturation, the excessive Pt formed metal nanoclusters. We previously proposed a universal strategy to prepare single-atom catalysts using bimetallic nanocrystals as promoters to spontaneously transform noble metals into single atoms on Al_2O_3 [41]. The metal single-atoms were anchored on the cationic defects in situ generated on the surface of the inverse spinel structure, hence enhancing thermodynamic stability of the catalyst. In addition to their unique advantages, the current preparation methods also have certain drawbacks, which include the difficulty in precisely controlling the reaction process and harsh reaction condition as well as the use of toxic organic solvents. These shortcomings limit the future practical applications of supported noble metal catalysts. Therefore, the development of more environmentally friendly reagents, along with more efficient and simpler methods, remains an area that requires further research.

2.2. Transition Metal Oxides, Composite Metal Oxides and Zeolite-Based Catalysts

Transition metal oxide catalysts have attracted extensive attention in the field of HVOCs elimination due to their lower cost, stronger resistance to halogen poisoning, and tunable redox properties and surface acidity, which have partially replaced noble metal catalysts. Recent research works have been focused on the preparation and application of porous transition metal oxides with high surface areas and porosity. Zeolite catalysts, with their good porosity and structures, tunable acidity, and high stability, often exhibit higher dispersion of the active components compared to single transition metal oxide catalysts, which is crucial for the enhancement in catalytic performance. Additionally, due to the unique synergistic effects between metals, composite metal oxides possess tunable compositions, structures, and electronic properties, which enable these materials to better face the unique challenges related to the elimination of HVOCs, i.e., catalyst poisoning, byproduct formation, and corrosivity [42–45].

The precipitation methods are categorized into direct precipitation, homogeneous precipitation, and co-precipitation. Direct precipitation refers to the process of obtaining the target oxide directly through precipitation. Homogeneous precipitation involves the dropwise addition of a precipitant solution to a metal salt solution under continuously stirring, allowing the precipitant to

 https://doi.org/10.53941/ges.2025.100012

slowly generate within the solution to eliminate its inhomogeneity. Co-precipitation refers to the addition of a precipitant to a solution containing multiple metal salts to obtain a homogeneous solution of several components, and after that the precipitation is thermally treated. The advantage of co-precipitation is that all of the metal ions in the solution are uniformly mixed at the molecular or ion level, resulting in the highly uniform dispersion of each active component at the atomic or nanoscale in the final catalyst. For example, Qiu et al. [42] prepared the Ce-doped MnO_x catalysts via the co-precipitation route so as to enhance redox ability and catalytic efficiency for *o*-dichlorobenzene oxidation of the catalysts. The precipitation methods are featured by their complexity, potential for impurity introduction, and the need for stringent operating conditions (e.g., specific water bath temperatures and pH values). Moreover, extensive water washing can lead to secondary environmental pollution.

Hydrothermal or solvothermal method is a synthesis technique conducted in a aqueous or organic solution. By selecting different solvents and controlling the synthesis parameters, transition metal oxide catalysts with specific morphologies (e.g., nanospheres, nanosheets, polyhedra, and etc.), high specific surface areas, and abundant pore structures can be prepared [2,22]. These characteristics facilitate exposure of the more active crystal facets, enhance redox properties of the metals, and improve the oxygen desorption and migration abilities, thus further boosting the catalytic efficiency. For example, Feng et al. [44] fabricated the Ce-Cu-W-O microspheres with surface-enriched W species and highly dispersed fine Cu species via a one-step hydrothermal route. Compared to the Ce-Cu-O catalysts, the microspherically morphological materials exhibit enhanced acidity and redox properties, which favor the improvements in deep oxidation ability and thermal stability for vinyl chloride (VC) removal. In addition, the hydrothermal method is a main means for synthesizing zeolite catalysts. In our previous work, we employed the hydrothermal method to prepare the Pt/Co-ZSM-5 catalyst featuring the Pt–O–Co and Co–O–Al species, which was enriched with the $Co^{3+}/Pt^{\delta+}$ sites and acidic sites, facilitating the activation of molecular oxygen and VOCs [47]. The in situ encapsulation of Co species promoted the close coupling of the acidic–redox centers and accelerated the oxidation of the intermediate species. Pt/Co-ZSM-5 exhibited good catalytic stability and strong resistance to poisoning by chlorine, water vapor, and sulfur dioxide. The encapsulation of Co inhibited the adsorption of SO_2 and promoted the decomposition of surface sulfate species due to its abundant surface acidity. Consequently, Pt/Co-ZSM-5 exhibited strong SO_2 tolerance, holding potential for practical applications. Similarly, Gołąbek et al. [48] introduced Ce into the BEA zeolite, endowing it with favorable structural properties (such as a well-developed mesoporous surface area, high dispersion of Ce^{3+}, high hydroxyl density (mainly Si–O(H)–Al), and enhanced Brønsted acidity). The optimized zeolite was conducive to the decomposition of trichloroethylene (TCE) into HCl and CO_2, while inhibiting chlorination reactions that produced tetrachloroethylene (PCE).

The sol-gel method is a preparation strategy, in which the metal inorganic or organic compounds undergo the sol-gelification and thermal treatment to form metal oxides. The core processes of the sol-gel method primarily include two key reactions: Hydrolysis and condensation. Metal alkoxides or inorganic salt precursors undergo hydrolysis in a solvent to form metal hydroxide compounds, which subsequently polymerize to generate a three-dimensional gel network structure. The desired product can be obtained after the thermal treatment. This method is typically conducted at room temperature or lower temperatures, which facilitates the generation of small-sized and highly active nanocatalytic materials. By loading CrO_x on the $LaSrMnCoO_6$ (LSMC) double perovskite that was fabricated via a simple sol-gel route, the as-obtained Cr/LSMC catalyst exhibited good reducibility, a large capacity of 1,2-dichloroethane (1,2-DCE) adsorption, and a number of surface active lattice oxygen species [45]. Wang et al. [43] fabricated the MnO_x-CeO_2 catalysts via the sol-gel route, and observed that a higher Mn/(Mn + Ce) molar ratio in the binary composite oxide could enhance chlorine resistance of the catalyst. However, some metal alkoxide precursors are expensive. The hydrolysis and condensation processes are difficult to control, the synthesis cycle is long, and the gel network is prone to shrinkage during the drying process.

3. Catalytic Applications for HVOC Elimination

3.1. F-VOCs

Fluorine is the most electronegative element, and its electronegativity is significantly different from that of carbon. The strong polarization of electron cloud towards F atoms results in highly polar covalent bonds, giving rise to a high energy of the C–F bond. Catalytic elimination is considered as an effective end-of-pipe treatment strategy for F-VOCs removal under mild conditions. Therefore, in the catalytic elimination of F-VOCs, fluorine is generally not an ideal leaving group. Typically, constructing the Lewis acid sites can accept electrons from the C–F bonds [6]. However, it was reported that the strong acid sites could also abstract F^- from dichlorodifluoromethane (CFC-12), giving rise to an increase in F^- concentration on the catalyst surface, which in turn promoted formation of the trichlorofluoromethane (CFC-13) undesired product [4,49]. In addition, the strong reactivity of F_2 and HF leads to the formation of stable metal fluorides at the active sites (typically acidic sites on metal oxide surface or metal ions) of catalysts, in which the formed metal fluorides permanently occupy or destroy the active centers, thus resulting in rapid deactivation of the catalysts [49,50].

Previous studies revealed that in the presence of water vapor, there was a reversible reaction (M–OH + HF ⇋ M–F + H_2O) between surface oxygen/hydroxyl groups and fluorine on the catalyst. It might be due to this reversible reaction that fluorine species were less likely to deposit on the catalyst surface [50], but water often competes with reactants for adsorption on the surface of catalysts [51]. Therefore, the effect of water on catalytic elimination of the F-VOCs requires further investigation. In addition, the secondary pollution caused by the generated fluorinated byproducts and the involved reaction mechanisms still remain unclear. Hence, we categorize the F-VOCs into perfluorocarbons (PFCs), CFCs, and HFCs based on their elemental compositions and summarize the research progresses on their catalytic elimination. Table 2 provides a comparison on catalytic activity of various catalysts for the removal of F-VOCs reported in the literature.

Table 2. Catalytic performance for F-VOCs elimination of the catalysts reported in the literature.

F-VOCs	Catalyst	SV (mL/(g·h))	Concentration	$T_{>95\%}$ (°C)	Stability (h)	Ref.
CF_4	S-Al_2O_3@ZrO_2	1000	2500 ppm	580	10	[5]
CF_4	γ-Al_2O_3	2000	5000 ppm	700	6	[52]
CF_4	Ce10%-$AlPO_4$	420	5000 ppm	700	90	[53]
CF_4	θ-Al_2O_3	2000	5000 ppm	750	100	[54]
CF_4	Hf/Al_2O_3	2000	2500 ppm	650	16	[55]
CF_4	Zn/Al_2O_3	2000 (h^{-1})	7000 ppm	750	70	[56]
CF_4	0.1-ZnAl	0.141 (h^{-1})	6700 ppm	700	30	[57]
CFC-12	WO_3/TiO_2	6000	1000 ppm	255	120	[17]
CFC-12	S-Ru/3DOM VTO	40,000	600 ppm	285	50	[49]
CFC-12	MoO_3/ZrO_2	300	4 vol%	400	–	[58]
CFC-12	$AlPO_4$	533	1.25 vol%	400	–	[59]
CFC-12	Mo_2O_3/ZrO_2	720	10 vol%	250	100	[60]
HFC-134a	$Zr_3(PO_4)_4$	467	5000 ppm	450	–	[14]
HFC-134a	$CePO_4$-$AlPO_4$	467	5000 ppm	450	–	[14]
HFC-134a	γ-Al_2O_3	300	20 vol%	600	24	[61]
HFC-134a	Mg/Al_2O_3	5000	2 vol%	600	6	[62]
HFC-134a	S-Ga/Al_2O_3	2362 (h^{-1})	1 vol%	500	30	[63]

3.1.1. PFCs

CF_4 is one of the most extensively studied types among all of the PFCs due to its highly symmetrical molecular structure with the C–F bond energy being 543 ± 4 kJ/mol. Catalytic hydrolysis, which is operationally simple and generates harmless end products, is one of the most extensively studied processes [52]. Takita et al. first investigated the catalytic hydrolysis of CF_4 over the $AlPO_4$-based catalysts [53]. The addition of a rare earth element (e.g., Ce, La, Pr or Nd) enhanced the crystallinity of $AlPO_4$, thus improving fluorination resistance of the catalysts. Moreover, the introduction of water enhanced the concentration of hydroxyl groups on the catalyst surface. Al_2O_3-based catalysts are usually used in catalytic CF_4 hydrolysis due to its easy availability and simple surface structure. Zhang et al. [54] compared the stability of different crystal forms of Al_2O_3 for catalytic CF_4 hydrolysis, and proposed that the alumina with higher-order polymorphs exhibited good resistance to HF corrosion. To further investigate the role of catalysts, possible fluorination reactions, and formation of related products in catalytic CF_4 hydrolysis, it is highly required to explore the possible reaction pathways of catalytic CF_4 hydrolysis and precisely identify the active sites in catalysts.

In the activation of PFCs, the unique stability of C–F bonds means that F is not generally an ideal leaving group. Typically, constructing the active sites with strong Lewis acid effects can facilitate activation of the fluorinated compounds by accepting electrons from F atoms [6]. EI-Bahy et al. [64] designed a series of binary metal oxides containing alumina (e.g., Ga–Al, Ni–Al, Zn–Al, Zr–Al, and Cr–Al) for the catalytic hydrolysis of CF_4, and found that some of these materials facilitated the hydrolysis of CF_4 to produce CO_2. Over the Ga–Al binary oxide catalyst, the CF_4 decomposition efficiency exceeded 90% within 20 h of reaction at 677 °C. The number of Lewis acid sites followed the order same as catalytic activity. It was proposed that cleavage of the C–F bond in CF_4 by the Lewis acid sites was the rate-determining step of CF_4 hydrolysis. CF_4 hydrolysis over the catalyst was divided into two steps: (i) Fluorination of the catalyst surface by CF_4 and (ii) recovery of surface fluorides to the surface oxides through hydrolysis and defluorination. Meanwhile, surface carbon species were oxidized to CO_2. Since surface fluorides are inactive for the defluorination reaction, the formation of fluorides can slow down the hydrolysis reaction. Therefore, adsorption and activation of the fluorine species on the catalyst surface are the key factors determining the catalytic performance for the hydrolysis of CF_4. Moreover, surface fluorides can be promptly hydrolyzed by water to promote the continuous progress of catalytic CF_4 hydrolysis.

Figure 1 illustrates the spatial structure of the CF_4 molecule, its frontier molecular orbitals, and the changes

in the density of states of the active centers on the Al_2O_3 catalyst [55]. Stability of the CF_4 molecule can be assigned to its tetrahedral configuration. The molecular orbitals of CF_4 are composed of the sixteen orbitals from the four F atoms and the four orbitals from the C atom (Figure 1a). The s electrons from the F atoms are distributed across two nested energy level orbitals ($2t_2$ and $3a_1$), which are primarily unreactive. In addition, the combination of F 2p orbitals with C 2s and 2p orbitals generates five bonding orbitals located near the Fermi level. The antibonding orbitals of CF_4 are entirely composed of F 2pσ orbitals and C 2p orbitals. Analysis of the partial charge density of the frontier orbitals reveals that the HOMO is primarily located on the F atoms, whereas the LUMO is mainly situated between the C and F atoms. Hence, the activation of CF_4 originates from the transfer of electrons from its HOMO to the active center, which necessitates a strong electron-accepting capability at the active center. The (110) crystal plane of γ-Al_2O_3 features three distinct coordination environments for Al atoms: One is trivalent, but two are quadrivalent. For the (100) crystal plane, there are four different types of pentavalent Al atoms [52]. The investigations on both computational modeling [65] and experiments [66] on Al_2O_3 reveal that the (110) crystal plane is the most active, with the 3-coordinated ($1Al_{3c}$) site showing a good catalytic activity for CF_4 decomposition, a CF_4 adsorption energy of –0.44 eV, and an Al–F bond length of 0.206 nm [55]. In contrast, the average adsorption energy of CF_4 at 4-coordinated Al sites ($2Al_{4c}$ and $3Al_{4c}$) is 0.2 eV higher than that at $1Al_{3c}$, and the Al–F bonds are longer, which indicates a significantly weaker adsorption of CF_4 at these sites (Figure 1b). Zhang et al. identified trivalent Al atoms as the dominant active sites for catalytic reactions, and concluded that these sites could effectively activate CF_4 by stretching the C–F bonds [52]. Lewis acid center is a key factor in activating the C–F bonds that directly influences the catalytic activity of catalytic CF_4 hydrolysis. Acidity of the Lewis acid sites on Al_2O_3 could be determined on the basis of the energy level position of unoccupied orbitals in the density of states. The proximity of unoccupied orbitals on Al atoms to the Fermi level determined the strength of electron-accepting ability. Therefore, strength of the Lewis acid sites could be measured by the distance between unoccupied orbitals and Fermi level. The highly active $1Al_{3c}$ site exhibits unique anti-bonding orbital characteristics. The $1Al_{3c}$ site shows the biggest peak on the anti-bonding orbital closest to the Fermi level, indicating the increased electron-accepting ability. As shown in Figure 1c, after CF_4 adsorption, the electron density in the anti-bonding orbital of the $1Al_{3c}$ site significantly decreases, implying that the active site anti-bonding orbital is occupied. The activation of CF_4 involves an electron transfer from the HOMO to the anti-bonding orbital of the Al active site. Since most Al sites on Al_2O_3 lack the ability to activate CF_4, however, this hinders the overall activation of CF_4 required on the surface of the catalyst. Designing the alternative strategies to control anti-bonding orbital occupancies can improve adsorption and activation of PFCs. Therefore, Luo et. al. further introduced Zr and Hf to enhance CF_4 adsorption [55]. The occupancy of anti-bonding orbitals at Zr and Hf active sites results in enhanced electron-accepting ability from CF_4, significantly improving the electron interaction between the active sites and CF_4. The CF_4 conversions of 54.5 and 100% at 650 °C were achieved over the as-prepared Zr/Al_2O_3 and Hf/Al_2O_3 catalysts, respectively.

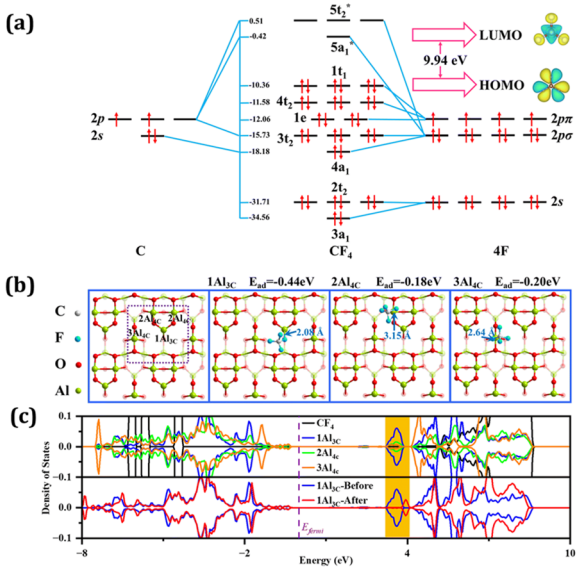

Figure 1. (**a**) Schematic diagram of the CF_4 molecular orbital energy levels and frontier orbitals (HOMO and LUMO), (**b**) atomic models of different Al sites and CF_4 adsorption energy at the Al_2O_3 surface, and (**c**) the p orbital density of states at different Al sites and 3-coordination Al sites before and after CF_4 adsorption. Gray spheres represent carbon (C) atoms, blue spheres represent fluorine (F) atoms, red spheres represent oxygen (O) atoms, and green spheres represent aluminum (Al) atoms [55]. Copyright 2023, Royal Society of Chemistry.

In addition to the key role of trivalent Al in Al_2O_3 as the Lewis acid site in the activation of C–F bonds, proton donors can also interact with the C–F bonds [67]. For instance, the interaction of hydroxyl groups with the C–F bonds facilitated the chemical decomposition of fluorine [68]. Strength of the interaction with the C–F bonds is influenced by the type of proton donor. Therefore, by modulating the proton donors on the surface of the catalyst, the C–F bonds can be further activated. Chen et al. [5] proposed an approach to effectively activate the C–F bonds using the protonated sulfate (–HSO_4)-modified Al_2O_3@ZrO_2 (S-Al_2O_3@ZrO_2) catalysts, which could efficiently decompose CF_4. As shown in Figure 2a, the S-Al_2O_3@ZrO_2 catalyst containing –HSO_4 showed an excellent CF_4 hydrolysis activity, with the complete

decomposition of CF_4 at 580 °C and a turnover frequency of 8.3 times higher than that of the Al_2O_3@ZrO_2 catalyst. The enhanced interaction between the introduced proton donor (–HSO_4) and the C–F bond played a critical role in improving CF_4 hydrolysis activity. The interaction between –HSO_4 and the C–F bonds was stronger than that between –OH and the C–F bonds, effectively activating the C–F bonds and thus promoting CF_4 decomposition. On the other hand, water, which is one of the reactants in catalytic CF_4 hydrolysis, can provide hydroxyl groups and proton for the reaction. However, the presence of H_2O leads to competitive adsorption with CF_4, which is detrimental to the reaction to some extent. Luo et al. [69] used the constrained ab initio molecular dynamics simulations and in situ experiments to further clarify the mechanism of CF_4 decomposition over alumina, and emphasized the key role of surface hydroxyl groups. Surface –OH groups could reduce the reaction free energy for cleavage of the C–F bond from 1.69 to 1.34 eV. As depicted in Figure 2b, the resulting *F and *CF_3 subsequently anchor near the trivalent Al and O sites, respectively, and the subsequent process involves a Mars–van Krevelen (MvK) mechanism with the involvement of lattice oxygen in the reaction. *OCF_3 extracts lattice oxygen, leading to formation of the temporary oxygen vacancies, which are rapidly repaired by the surface hydroxyl groups. *OCF_3 undergoes defluorination to generate *OCF_2, which further decomposes to *OCF. In the final separation stage, *CO dissociates into the CO molecules. At high temperatures, CF_2O and CO are observed to transform into the final products (i.e., CO_2 and HF). H_2O primarily replenishes the surface –OH groups, rather than directly involving in the decomposition reaction. A high density of the surface –OH groups is conducive to the initial C–F bond cleavage and self-healing of oxygen vacancies. This process highlights the dynamic interaction on the catalyst surface.

In the hydrolysis of CF_4, once the first C–F bond in CF_4 is cleaved, the remaining C–F bonds in CF_4 undergo rapid dissociation and subsequent hydrolysis. It is noteworthy that the C–F bonds in CF_4 are more stable than those in the formed intermediates after partial decomposition. Hence, activation of the C–F bond is considered as the rate-determining step in CF_4 hydrolysis. Although constructing the appropriate active sites can significantly improve catalytic activity, enhancing the migration capability of fluorine species on the surface of the catalyst and its fluorine resistance are even more important in view of catalyst stability. Introducing Zn and Ni on the surface of Al_2O_3 can generate the corrosion-resistant $ZnAl_2O_4$ and $NiAl_2O_4$ on the catalyst surface, thereby increasing the catalyst stability [56]. However, such an introduction action also leads to the depletion of surface acid centers, resulting in declined catalytic CF_4 removal activity. Therefore, a rational strategy for the regulation of catalyst surface structure should have dual functions: Improving the catalyst durability and participating in the reaction as an active component. Jeon et al. [57] modulated the molar ratio of Zn/Al, and found that at Zn/Al = 0.1, the spinel structure of $ZnAl_2O_4$ with a core-shell morphology was selectively formed on the surface of Al_2O_3. Compared to γ-Al_2O_3, the Lewis acid sites in $ZnAl_2O_4$ were beneficial for the adsorption of CF_4 but weakened the adsorption of H_2O, thereby decreasing the negative effect of H_2O. Despite the overall reduction in amount of the Lewis acid sites after Zn doping, the Zn-doped γ-Al_2O_3 catalyst showed remarkedly enhanced catalytic performance. Moreover, the coating of $ZnAl_2O_4$ on the γ-Al_2O_3 microcrystals prohibited the phase transformation of γ-Al_2O_3 to α-Al_2O_3, hence enhancing stability of the catalyst. In addition to catalyst deactivation caused by the strong electronegativity of fluorine species, the elimination efficiency of PFCs (e.g., CF_4) drops sharply in the initial stage of catalytic hydrolysis. Wang et al. [70] proposed that the formation of carbonaceous (*COO) species was responsible for the decline in activity, with the adsorption configuration of the *CFOH intermediate being crucial for the generation of these toxic *COO species. By introducing the Ni sites with strong adsorption ability, the *CFOH at the Al active sites could be transferred to the adjacent Ni sites, thus preventing the formation of the toxic *COO species. The defluorination of the *CFOH species at the Ni active centers formed the *CO species, which was ultimately oxidized to CO_2, hence detoxifying the Al_{III} active centers. Over the Ni/γ-Al_2O_3 catalyst, a complete conversion of CF_4 was achieved at 570 °C after over 300 h of reaction.

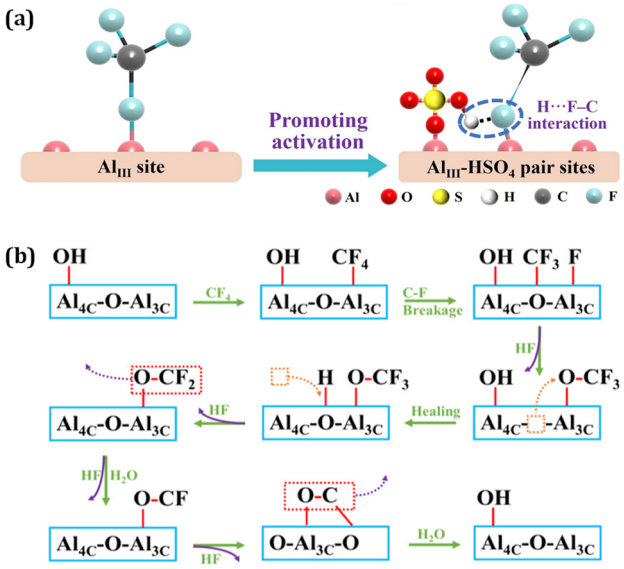

Figure 2. (**a**) Schematic illustration of –HSO_4 proton donor promoting the C–F bond activation for CF_4 decomposition [5]. Copyright 2023, PNAS. (**b**) Schematic diagram of the complete reaction pathway of CF_4 catalytic hydrolysis on γ-Al_2O_3 [69]. Copyright 2024, American Chemical Society.

 https://doi.org/10.53941/ges.2025.100012

3.1.2. CFCs

Catalytic elimination is an effective pathway for the complete destruction of CFCs, which refers to the oxidation of CFCs with O_2 over catalysts to produce CO_2, CO, HCl, and HF [4]. Previous research works on catalytic removal of CFCs have primarily been focused on the acidic catalysts, since the introduction of acid sites facilitates the adsorption and activation of CFCs [58–60,71]. Usually, γ-Al_2O_3 with a high specific surface area and a suitable surface Lewis acidity is a commonly used catalyst or support, and its surface acid sites can serve as the active sites for CFCs activation. In the catalytic elimination of CFC-12 over γ-Al_2O_3, HF interacted with γ-Al_2O_3 to form the low-surface-area and inactive α-AlF_3, giving rise to a rapid decline in catalytic activity. Ng et al. [72] reported the catalytic removal of CFC-12 over the $CrCl_3$/γ-Al_2O_3 catalyst. The interaction of $CrCl_3$ with HF generated CrF_x, which inhibited the reaction between Al_2O_3 and HF, thus slowing down the catalyst deactivation. The strategy of modifying the catalyst surface with transition metal chloride (which formed the transition metal fluoride phase on the Al_2O_3 surface) helps the $CrCl_3$/γ-Al_2O_3 catalyst to resist deactivation. However, the transition metal chloride could decrease activity of the fresh catalyst. To simultaneously enhance activity and stability of the modified catalysts, some researchers fabricated numerous SO_4^{2-}-promoted solid acid catalysts, and pointed out that the catalytic activity dropped in the sequence of SO_4^{2-}/ZrO_2 > SO_4^{2-}/TiO_2 > SO_4^{2-}/SnO_2 > SO_4^{2-}/Al_2O_3 [17]. In the sulfate-promoted TiO_2 sample, a strong interaction between sulfate anions and titanium cations resulted in high catalytic performance and good resistance [16]. The partial substitution of surface oxygen and/or hydroxyl groups by the more electronegative fluorine can increase the polarity of the metal oxide lattice, thereby enhancing the nearby Brønsted and Lewis acidity, which in turn improves the catalytic activity for CFCs elimination [49,50]. Therefore, fluorine can influence catalytic activity of metal oxides by polarizing the catalyst lattice. However, such a fluorination phenomenon inevitably leads to catalyst deactivation. Greene et al. [50] suggested that the presence of H_2O endowed the TiO_2 catalysts with good CFCs elimination activity and CO_2 selectivity, with water vapor being a necessary condition for generating the stronger acidity. The sources of the Lewis and Brønsted acid sites in TiO_2 and the role of water are well-known. Coordinated unsaturated cations on the TiO_2 surface may accept lone electron pairs from adsorbed molecules, hence acting as the Lewis acid centers. In a hydroxylated environment, the dissociative adsorption of H_2O at the coordinated unsaturated cations and anions of the catalyst can also generate the Brønsted acid centers. Therefore, the hydroxylated TiO_2 has more Brønsted acid sites than the dry (dehydroxylated) TiO_2. It is generally believed that after CFC-12 is adsorbed at the acid centers, it interacts with the surface –OH groups to form the intermediates (e.g., $COCl_2$ and COFCl) that then react with H_2O to generate the fully oxidized products. It has been confirmed that the active oxygen species can be generated under the conditions where water and oxygen coexist. The –OH groups on the surface of the catalyst are replenished through the dissociative adsorption of water on the catalyst.

3.1.3. HFCs

Given the ozone-depleting effects of CFCs, HFCs have gained a significant attention as substitutes for CFCs, but the GWP of HFCs remains high. Furthermore, the production of HFCs generates additional fluorinated byproducts. For example, the increased demand for 1,1,1,2-Tetrafluoroethane (HFC-134a) results in the formation of substantial amounts of the CF_3CH_3 byproduct [73]. HFC-134a is widely used as a refrigerant in domestic refrigerators and air conditioners as well as in the foam industry, which serves as an ideal substitute for CFC-12.

Catalytic elimination refers to the complete removal of HFC-134a over a catalyst in the presence of O_2, resulting in the formation of CO_2, HF, and/or F_2. Compared to catalytic pyrolysis in the absence of oxygen, the addition of oxygen significantly reduces the Gibbs free energy barrier for HFC-134a decomposition and decreases the formation of secondary fluorinated byproducts. Takita et al. [14] investigated the elimination of HFC-134a over several phosphate catalysts. The temperatures required for achieving a 100% conversion of HFC-134a over $Zr_3(PO_4)_4$, $AlPO_4$, and BPO_4 were 475, 500, and 700 °C, respectively. The oxidative properties of metal phosphates were insufficient for the complete removal of HFC-134a. The doping of Ce enhanced the catalytic activity of $AlPO_4$ for HFC-134a elimination. The decomposition rate of HFC-134a was proportional to the concentration of surface hydroxyl groups rather than their quantity on the surface of the catalyst. Complete removal of HFC-134a requires both oxidation and hydrolysis reactions. Han et al. [61] studied the catalytic elimination of HFC-134a over Na_2CO_3, CaO, $CaCO_3$, and two γ-Al_2O_3 catalysts with different surface areas, among which the γ-Al_2O_3 catalyst with a higher surface area exhibited the best activity for HFC-134a elimination. Fluorination on the surface of alumina generated the low-activity AlF_3, giving rise to the gradual catalyst deactivation. Introducing H_2O to the reaction system enhanced the selectivity towards HF, preventing the phase alteration from Al_2O_3 to AlF_3, hence significantly improving the catalytic stability [13,61,62]. Furthermore, the acid-modified S/Ga-Al_2O_3 catalysts derived from the co-precipitation and impregnation routes maintained a 80% conversion of HFC-134a for over 30 h of on-stream reaction at 450 °C [63]. This result was attributed to

retention of the partially reduced Ga species and promotion of the Lewis acidity on the catalyst surface by the sulfuric acid treatment. To achieve efficient catalytic HFC-134a elimination, the active oxygen species play a critical role in the oxidation reaction, and the addition of water can significantly enhance the catalyst lifespan, even co-generating the new active oxygen species with oxygen. Therefore, to achieve the goal of efficient HFC-134a removal, it is important to develop the suitable catalysts to increase the concentration of surface –OH groups and reactive oxygen species in the reaction system.

3.2. Cl-VOCs

Cl-VOCs are classified as highly toxic pollutants by most countries owing to their strong toxicity, high chemical stability, and low biodegradability. Catalytic oxidation exhibits excellent catalytic efficiency in eliminating low-concentration Cl-VOCs. Organic chlorine can be oxidized into inorganic HCl and Cl_2. Typically, complete elimination of Cl-VOCs can be achieved in the range of 200–500 °C by strictly controlling the reaction conditions (such as space velocity (SV)); otherwise, more toxic substances like polychlorinated biphenyls and dioxins may be generated [1,2]. The catalytic oxidation of Cl-VOCs involves complex reaction mechanisms or pathways, including the generation of highly reactive chlorine species (such as Cl_2 and Cl•) and byproducts, which pose significant challenges for the rational designing of efficient catalysts [74]. Thus, a deep understanding on catalytic strategies and reaction mechanisms is the key to achieving a higher low-temperature removal efficiency. Reducing the residence time of inorganic chlorine species during the catalytic process is a key to inhibiting catalyst poisoning and minimizing the formation of byproducts. The synergistic effect of acidity and redox ability is crucial for the enhancement in strong degradation ability of the catalyst. Surface oxygen species and oxygen mobility are key factors affecting the catalyst redox ability. In addition, maintaining sufficient active sites is also important for the catalytic oxidation of Cl-VOCs [2]. Based on their molecular structures, Cl-VOCs can be categorized into chloroalkanes, chloroolefins, and chlorinated aromatics. This section will provide a detailed introduction of these Cl-VOCs. Table 3 summarizes the various catalysts used for Cl-VOCs removal reported in the literature.

Table 3. Catalytic performance for Cl-VOCs elimination of the catalysts reported in the literature.

Cl-VOCs	Catalyst	SV (mL/(g · h))	Concentration	$T_{50\%}$ (°C)	$T_{90\%}$ (°C)	Ref.
1,2-DCE	RuP/3DOM WO_x	40,000	1000 ppm	300	353	[21]
1,2-DCE	Ru/HPW-TiO_2	40,000	1000 ppm	–	300	[24]
1,2-DCE	5Fe-CeO_2-HT	15,000	250 ppm	–	237	[75]
1,2-DCE	0.91RuCo/HZSM-5	20,000	1000 ppm	238	281	[76]
1,2-DCE	Cr/SMC-F	36,000	1000 ppm	177	266	[77]
DCM	Pt/Al_2O_3	20,000 (h^{-1})	1000 ppm	–	<340	[33]
DCM	Ru@Silicalite-1-Sn-50	40,000	500 ppm	270	325	[23]
DCM	Ce/TiO_2	30,000 (h^{-1})	1000 ppm	–	<355	[78]
DCM	PO_x-CeO_2-0.2	15,000	500 ppm	–	330	[79]
TCE	0.98Ru/3DOM SnO_2	40,000	1000 ppm	274	300	[20]
TCE	2.85AuPd$_{1.87}$/3DOM CeO_2	20,000	750 ppm	330	415	[80]
TCE	Pt_3Sn(E)/CeO_2	40,000	100 ppm	22	263	[81]
TCE	3DOM 5.5Cr_2O_3-CeO_2	20,000	750 ppm	214	255	[82]
CB	Ru/MoO_x/HZSM-5	20,000	1000 ppm	330	370	[22]
CB	MnO_x-CeO_2	15,000 (h^{-1})	1000 ppm	<200	<250	[43]
CB	PtBEA75	26,580	2000 ppm	300	<350	[83]
CB	$Cu_{0.15}Mn_{0.15}Ce_{0.85}O_x$	30,000 (h^{-1})	600 ppm	–	255	[84]
CB	2.4W/CeO_2	30,000	1000 ppm	266	339	[85]

3.2.1. Chloroalkanes

Chloroalkanes possess relatively simple structures, comprising three representative chemical bonds (i.e., C–C, C–H, and C–Cl). DCM is one of the most stable chloroalkanes, which is difficult to naturally degrade in the environment. The Ce-based catalysts with abundant oxygen vacancies and redox abilities exhibit excellent catalytic oxidation performance. Cao et al. [78] studied the oxidation of DCM over the Ce/TiO_2 catalyst, and observed that the Cl species tended to strongly adsorb and accumulate on the surface of TiO_2, eventually giving rise to catalyst deactivation. The loading of CeO_2 on TiO_2 could rapidly remove the surface Cl species, reducing their poisoning effect and enhancing activity and stability of the catalyst. The zeolitic molecular sieves with developed pore structures, good thermal stability, and excellent ion-exchange ability are widely used as catalysts or catalyst supports for Cl-VOCs oxidation. Wu et al. [23] synthesized the Sn-doped silicalite materials via a hydrothermal route. The incorporation of Sn effectively anchored the Ru atoms, leading to the atomic dispersion of Ru and the generation of oxygen vacancies. The Ru@silicalite-1-Sn

 https://doi.org/10.53941/ges.2025.100012

catalyst with the closely coupled redox and acidic centers showed a strong electronic transfer through the Sn–O–Si bonds, increasing the Lewis acidity and thus promoting the oxidation of dechlorination intermediates. Metal-organic frameworks (MOFs) are a class of highly ordered porous materials with different topological structures formed by connecting metal centers with organic ligands through coordination bonds [29]. By judiciously selecting the MOF precursors and rationally designing the pyrolysis conditions, MOFs can be used as a promising sacrificial template for the precise construction of metal oxides. Deng et al. [86] doped Ti^{4+} into the CeO_2 lattice (CeTiO-x) by calcining the bimetallic TiCe-based MOFs to effectively oxidize DCM. The results indicated that this design could generate a large number of Ce^{3+}/Ce^{4+} redox pairs stabilized by Ti^{4+}, thus enhancing CO_2 selectivity. The reversible Ce^{4+}/Ce^{3+} redox couple, combined with the preferential adsorption of chloride ions at the Ti^{4+} sites, endows the CeTiO-x catalyst with excellent catalytic performance and resistance to chlorine and moisture. Additionally, the metal centers in MOFs are often unsaturated due to the presence of small-molecule solvents, making them highly suitable as active sites. Their high surface areas and porous structures facilitate the high dispersion of noble metals and the good contact between VOCs and active sites. In one of our previous works, we first reported the direct use of MOFs rather than MOF derivatives for the catalytic elimination of Cl-VOCs [29]. Ru-UIO-66S, which was prepared with BDC−SO_3Na as the organic ligand and rich in Brønsted acid hydroxyl groups, exhibited good photocatalytic Cl-VOCs oxidation activity and high HCl selectivity. 1,2-DCE is an intermediate for polyvinyl chloride production and one of the most important Cl-VOCs in industrial flue gas emissions. Achieving environmentally friendly catalytic elimination of 1,2-DCE at low temperatures is a current research focus for many researchers [1]. Wang et al. synthesized the two-dimensional Fe-doped CeO_2 nanosheets using the hydrothermal, co-precipitation, and solvothermal (ST) methods, and applied them to the oxidative removal of 1,2-DCE [75]. The results indicated that the 5 wt% Fe-CeO_2-ST catalyst showed a superior activity and lower selectivities towards polychlorinated hydrocarbons, which were attributable to its higher concentrations of oxygen vacancies and active oxygen species. The addition of VO_x or RuO_2 to Fe-CeO_2-ST further enhanced the stability and selectivities for 1,2-DCE oxidation. In the oxidation of 1,2-DCE, microporous zeolites with large surface areas are commonly employed as supports. In one of our previous works, we studied the catalytic performance of microporous HZSM-5-supported RuCo bimetallic nanoparticles (RuCo/HZSM-5) catalysts for the oxidation of 1,2-DCE. RuCo/HZSM-5 showed a good catalytic activity and an apparent activation energy of 36 kJ/mol at a SV of 20,000 mL/(g · h) [76]. In the bimetallic catalysts, the RuO_2 species were predominant, and Co doping increased the length of the Ru–O bond. The good chlorine resistance was associated with the strong interaction between highly dispersed Ru species and CoO_x through formation of the Ru–O–Co bonds and the fact that chlorine preferentially is adsorbed at the Co sites, leaving the active Ru species unaffected by chlorine poisoning. Therefore, the catalysts used for Cl-VOCs oxidation should possess strong redox ability, appropriate acidity, good Cl-VOCs adsorption performance, highly dispersed active components, and strong metal–support interactions.

It is generally believed that hydroxyl radicals on the catalyst directly participate in the oxidation process. 1,2-DCE reacts with hydroxyl groups to form acetaldehyde, which subsequently generates methoxy and formic acid, with the final oxidation of the formate species to CO_x by the hydroxyl radicals [87]. Yang et al. [88] suggested that rutile TiO_2(110) had the surface-bridging oxygen atoms rich in electrons, which facilitated cleavage of the C–Cl bond. The strong acidity formed by the reaction with sulfate can better promote chlorine dissociation. In one of our previous works, we proposed that the Mo–O(H)–Al structure in Ru/MoO_x/HZSM-5 synergized with the acidic Si–OH–Al structure in HZSM-5, making it easier for water vapor adsorbed at oxygen vacancies of the catalyst to be activated into the bridging hydroxyl groups [22]. The dissociated H_2O species reacted with the adsorbed oxygen species to generate the active *OOH species, thereby promoting the deep oxidation of the intermediate products. Yin et al. [89] used the density functional theory (DFT) methods to conduct in-depth calculations of the fundamental steps in the catalytic oxidation of 1,2-DCE, determining the lowest energy pathway for 1,2-DCE oxidation on the CeO_2(111) surface. Oxygen vacancies are the primary adsorption centers for DCE oxidation. 1,2-DCE first loses two chlorine atoms at oxygen vacancies to generate the CH_2CH_2 fragments, followed by dehydrogenation and C–C bond cleavage, and is ultimately oxidized to CO_2 and H_2O by the surface lattice oxygen or adsorbed oxygen species. Oxygen vacancies play a crucial role in C–Cl bond cleavage, as one of the two additional surface electrons it provides can be transferred to the adsorbed Cl, rendering it to be negatively charged and leading to a strong electrostatic interaction with nearby Ce ions, hence facilitating the C–Cl bond cleavage. Due to the lower energy barrier of the C–Cl bond and higher potential energies of the C–C and C–H bonds, the former bond consistently cleaved prior to the latter two bonds. Dechlorination, dehydrogenation, and C–C bond cleavage takes place sequentially. Tian et al. [77] proposed two pathways of catalytic 1,2-DCE removal: cleavage of the C–Cl bond to produce VC (with the release of HCl) and breaking of the C–C bond to produce CH_3Cl. Lattice oxygen primarily participates in redox reactions through the MvK mechanism by interacting with the adsorbed dichloroethane and other chlorinated molecules. Subsequently, lattice oxygen and electrons are

transferred with the replenishing of the active oxygen species. Fei et al. [90] found that 1,2-DCE was sequentially converted into carbenes (COO^-), alcohols (C_2H_6O), and acetic acid (CH_3COOH) with the rise in temperature. Alcohols are the typically detected intermediates formed on the catalysts with weaker redox ability. Yang et al. [91] reported that –OH groups and oxygen in HZSM-5 transformed 1,2-DCE into chlorohydrocarbons, CH_3CHO, and CH_3COOH through protonation and nucleophilic oxidation. Finally, the above intermediates were totally converted into CO_x and H_2O (Figure 3) [79,92].

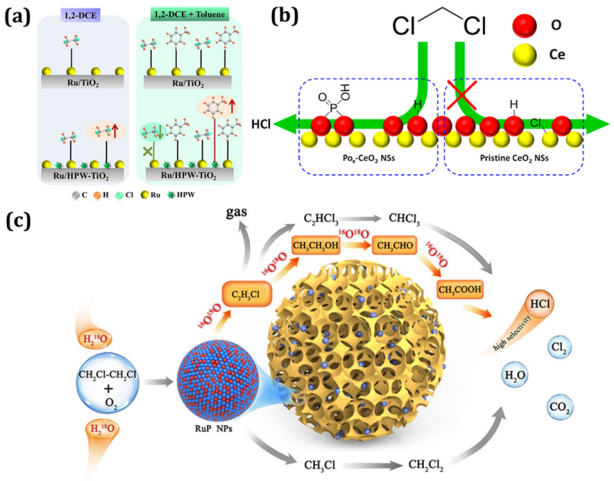

Figure 3. (**a**) The diagram of 1,2-DCE and toluene adsorption behavior on the catalysts [24]. Copyright 2022, American Chemical Society. (**b**, **c**) possible reaction pathways of 1,2-DCE oxidation [21,79]. Copyright 2018, American Chemical Society. Copyright 2021, American Chemical Society.

3.2.2. Chloroolefins

Chloroolefins, which contain unsaturated the C=C bonds and π–π conjugated systems, exhibit strong stability due to the uneven distribution of electrons, and are prone to generating more polychlorinated byproducts during the catalytic oxidation processes [80]. Common chlorinated alkenes include VC, TCE, and PCE.

The perovskite-type oxide (ABO_3) catalysts are prepared after the high-temperature calcination processes, thereby exhibiting superior thermal stability and coking resistance. In the oxidation of VC, a VC removal of 90% can be achieved over the $LaMnO_3$ catalyst at 350 °C. Partial substitutions at the A and/or B sites and treatment with HNO_3 can alter the redox ability and acidity of the parent catalyst, hence enhancing the low-temperature activity and mitigating the formation of byproducts that induced the catalyst deactivation [93]. Giroir-Fendler et al. investigated the effect of B-site substitution with Co, Ni or Fe on catalytic activityof $LaMnO_3$ [94]. Due to the low porosity and poor redox properties of the perovskite catalysts, however, research on perovskite catalysts under low-temperature and mild conditions is relatively limited. TCE is a typical Cl-VOCs, which has been extensively studied for catalytic oxidation. We previously reported the preparation of Ru nanoparticles loaded on the three-dimensional ordered macroporous SnO_2 (Ru/3DOM SnO_2) using a polyvinyl alcohol-assisted $NaBH_4$ reduction strategy, and investigated their catalytic performance for the oxidative elimination of TCE and toluene [20]. It was found that 0.98Ru/3DOM SnO_2 showed the best catalytic performance and thermal stability. Chloroform, carbon tetrachloride, tetrachloroethylene, and trichloroacetaldehyde hydrate were detected as the main intermediates of TCE oxidation. The good catalytic performance of Ru/3DOM SnO_2 was associated with the –OH groups adsorbed at oxygen vacancies, large O_2 adsorption capacity, good low-temperature reducibility, and strong interaction between Ru nanoparticles and 3DOM SnO_2. The addition of H_2O suppressed the formation of C_2Cl_4 and reduced the formation of some byproducts (e.g., DCM, DCE, and CH_3COOH). In addition, H_2O introduction also promoted removal of the Cl species and generation of more HCl and less Cl_2. Moreover, the introduction of toluene into the TCE-containing atmosphere resulted in fewer organic chlorinated byproducts and more inorganic chlorine-containing products (i.e., HCl and Cl_2). Bimetallic catalysts have gained a significant research attention owing to their unique synergistic effects. The $Pt_3Sn(E)/CeO_2$ catalyst etched with HCl exhibited the Cl resistance superior to the Pt/CeO_2 catalyst due to the site-isolation effect [81]. The presence of aromatics markedly reduced the adsorption strength of TCE. The substantial surface adsorbed oxygen species formed on the electropositive platinum effectively promoted dissociation of the C–Cl bonds. The adjacent promoter (Sn–O) acted as an acid site, which maintained the reactivity of platinum by removing chlorine and minimizing the formation of polychlorinated byproducts (Figure 4a). Although base metal oxides generally exhibit lower catalytic performance than noble metals, they possess excellent redox properties and are more resistant to deactivation. We previously proposed that an appropriate amount of Cr_2O_3 doping in CeO_2 could enhance the surface adsorbed oxygen species concentration on 3DOM Cr_2O_3-CeO_2 and the low-temperature reducibility of this catalyst, thereby exhibiting higher TCE removal efficiency and better catalytic stability [82]. Base metal oxide catalysts have been considered to be potential alternatives to noble metal catalysts.

Here are some viewpoints regarding the pathway of catalytic TCE oxidation [2]. TCE is directly oxidized by the surface adsorbed oxygen species on the catalyst to form CO_x, with the Cl atoms being transferred to the catalyst to produce Cl_2, which then reacts with TCE to generate C_2HCl_5, ultimately yielding stable tetrachloroethylene upon dehydrochlorination. In contrast, TCE may be first adsorbed on the surface of the catalyst, followed by cleavage of the C–Cl bond and adsorption of the Cl atoms on the catalyst. The resulting CH_x species are further

 https://doi.org/10.53941/ges.2025.100012

converted to CO_2 and H_2O after its reaction with the active oxygen species. Given the strong carcinogenicity of VC and TCE and their subsequent bans, research on TCE degradation mechanisms is limited, and no consensus has been reached.

3.2.3. Chlorinated Aromatics

Chlorinated aromatics (e.g., chlorobenzene (CB) and polychlorinated biphenyls) have received a significant attention owing to their notable biological toxicity and environmental persistence. The unique π–π conjugated system, the ring structure composed of six carbon atoms, and the high energy of the C–Cl bonds endow these molecules to be exceptional chemical stability, making them be full of challenge in activation. CB is one of the most commonly studied compounds and is important precursor for the formation of dioxins. This section will summarize CB removal catalysts and reaction mechanisms separately.

The high stability of CB molecules and the involved issues (such as chlorine poisoning and formation of polychlorinated byproducts (e.g., polychlorinated biphenyls)) during the CB degradation processes severely limit practical applications of the catalytic oxidation technologies. Researchers have developed various catalytic systems and explored reaction mechanisms and optimization strategies in depth [2]. Noble metal Ru-based catalysts exhibited excellent performance in the combustion of CB [22]. The primary reason was that Ru could catalyze the Deacon reaction, where the adsorbed Cl species was oxidized by O_2 to form Cl_2, which was desorbed from the adsorption sites, hence enhancing the catalyst stability. Supports are typically chosen from metal oxides (e.g., Al_2O_3, CeO_2, and TiO_2) that inherently possess catalytic activities and have strong interactions with the active components. By altering the morphology of CeO_2, the interaction between Ru and CeO_2 could be further regulated [95]. Compared to the cubic and octahedral CeO_2, the rod-like CeO_2 enclosed by the (110) and (100) crystal facets could form a large number of the Ru–O–Ce-like bonds, increasing the Ru^{4+} species content and promoting the surface oxygen mobility, thereby reducing the activation energy for CB oxidation. This finding helps to understand catalytic behaviors of the noble metal catalysts supported on CeO_2 with different shapes or crystal facets in the oxidation of Cl-VOCs as well as to develop high-performance catalyst systems. When CB is catalytically combusted over Pt/Al_2O_3, the PtOCl species could catalyze the further chlorination of CB to produce polychlorinated benzenes [96]. Scirè Salvatore et al. [83] observed an increase in catalytic performance for CB oxidation after replacement of Al_2O_3 by HZSM-5, and a lower selectivity towards polychlorinated benzenes when zeolite was used as the support. This might be attributable to the "shape-selective effect" of zeolites, where the smaller channel size of zeolites could hinder further chlorination to form polychlorinated benzenes. Non-noble metal catalysts, which are relatively inexpensive, and abundant in resources, are potential alternatives to noble metal catalysts for Cl-VOCs combustion. The most commonly used non-noble metal catalysts for CB combustion are transition metal oxides, such as the oxides of Ce, Cr, and Mn as well as their composite oxides. He et al. [84] fabricated a mesoporous Cu–Mn–Ce–O composite material with a high surface area using the homogeneous co-precipitation method. Mn and Cu entered the fluorite-type CeO_2 matrix, inducing generation of a large quantity of oxygen vacancies. The presence of a significant amount of high-valent manganese (Mn^{4+}) species promoted generation of the reduced copper phase, exhibiting excellent catalytic activity. CB conversion could achieve 90% at 255 °C, with the CO_2 selectivity higher than 99.5%. Gu et al. [85] reported that loading WO_x on CeO_2 could significantly increase the oxygen vacancy concentration and acid strength due to the formation of a W–O–Ce-like structure, thereby showing an excellent CB removal efficiency. The introduction of water vapor at low temperatures is beneficial for enhancing the catalytic CB oxidation performance. Although hydroxyl groups facilitate the activation of the water adsorbed at the acid sites, the strong adsorption of the free water by hydroxyl groups inhibits formation of the surface oxygen species with increasing the temperature, hence suppressing the deep oxidation of CB.

It is generally believed that if the dissociated Cl can be promptly removed, the catalytic cycle is completed; otherwise, the Cl adsorbed on the catalyst leads to catalyst poisoning and an increase in side reactions (Figure 4b) [97]. Gao et al. [98] proposed that CB was ultimately converted to CO_2, HCl or Cl_2, and H_2O after the interaction of CB and the active oxygen species at the active sites of the catalyst. CB is first adsorbed on the catalyst and undergoes the nucleophilic substitution reaction (i.e., dechlorination (cleavage of the C–Cl bond)) to generate the phenolic species, which then undergo ring-opening of the benzene ring and oxidation to generate the key acetate intermediate. An increase in temperature promotes formation of the maleate species. Compared to the chlorinated species, these two intermediates have lower toxicity and are easier to transform, and further deep oxidation produces CO_2, while HCl may undergo the Deacon reaction to form Cl_2. Under dry conditions, the oxidation of CB gives rise to more byproducts intermediates (e.g., chlorinated ethoxy groups, phenols, and aldehydes). In the presence of H_2O, the co-activation of H_2O and O_2 can promote generation of the active oxygen species and hydroxyl radicals, facilitating electron transfer between the catalyst and the pollutant, and reducing the deposition of Cl elements, which is more beneficial for the adsorption and activation of CB as well as the deep oxidation of the formed intermediates (such as ring-opening of the benzene ring, transformation of the intermediate species to CO_2, and etc.), thus enhancing

catalytic performance and stability. Generally, the regeneration of catalyst activity is essential for extending catalyst lifespan and reducing production cost. Catalyst poisoning can be categorized into reversible and irreversible poisoning, with the strength of the interaction between the poison and the active component determining whether the catalyst can be regenerated [19]. The formation of coke and other intermediates (such as deposited halogenated species) can be removed by heating. However, it is important to note that the conventional thermal treatments to remove coke adsorbed on the catalyst surface can also lead to irreversible deactivation due to the agglomeration of surface metal particles. Long et al. [99] prepared a Ce–Zr co-modified monolithic Mn-based oxide catalyst via an one-pot solution combustion method, and found that the reduced activity of the catalyst could be partially regenerated when water vapor was introduced, as water inhibited the Deacon reaction and promoted removal of the chlorine species. In practical applications, catalyst deactivation and regeneration are interdependent and cyclical., activity and stability of the catalyst can be effectively restored through the rational regeneration routes, ensuring the continuous and efficient operation of the reaction process.

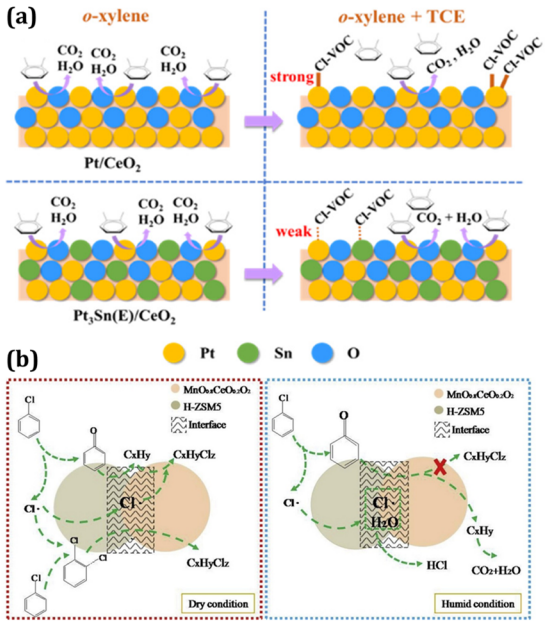

Figure 4. (**a**) Scheme of o-xylene and TCE adsorption on Pt/CeO_2 and $Pt_3Sn(E)/CeO_2$ [81]. Copyright 2022, American Chemical Society. (**b**) Proposed CB oxidation routes over $MnO_{0.8}CeO_{0.2}O_2$/H-ZSM5 and H-ZSM5 under dry and humid conditions [97]. Copyright 2016, Elsevier.

3.3. Br-VOCs

Br-VOCs are typical ozone-depleting substances, with bromine radicals being approximately 50 times more effective in ozone destruction than chlorine radicals. Methyl bromide (CH_3Br, MB) and dibromomethane (CH_2Br_2, DBM) are the primary categories of brominated hydrocarbons. The sources of Br-VOCs include natural biological emissions from the ocean, biomass burning, cooking processes, soil fumigation, quarantine fumigation, exhaust emissions from the PTA industry, methane bromination, and exhaust emissions from the bromination and oxidation of olefins. The complex exhaust composition of the PTA and potential methane halogenation industries have become focal points for exhaust treatment in recent years. In addition to Br-VOCs, these industry exhausts contain a higher proportion of traditional VOCs. Catalytic oxidation is universal, economical, and widely applicable, which is the mainstream pathway for eliminating exhaust gases related to Br-VOCs from industries. Similarly, the key issue for the catalytic oxidation of Br-VOCs remains development of the catalysts with high performance and stability. The catalytic oxidation of typical HVOCs involves the adsorption and dissociation of reactants at the surface hydroxyl groups/oxygen vacancies, followed by generating primary products with the assistance of acid centers/oxidation centers and ultimately complete oxidation to CO_2 and H_2O by the active oxygen species [1,2]. Two key issues exist in these processes: (i) The dissociated halogen atoms will lead to severe catalyst deactivation and may form highly toxic polyhalogenated byproducts; and (ii) the active metal sites can be partially occupied by halogen atoms, making it extremely difficult for O_2 to participate in the oxidation reactions at low temperatures. The Ru/TiO_2 catalyst was developed due to its unique ability to undergo the Deacon-like reaction, which could convert the free bromine species to Br_2, thereby initially suppressing the halogen deactivation at higher temperatures [27]. However, enhancing the low-temperature redox property of the catalyst still remains a key challenge. Table 4 provides a comparison on catalytic activity of various catalysts for the removal of Br-VOCs reported in the literature.

 https://doi.org/10.53941/ges.2025.100012

Table 4. Catalytic performance for Br-VOCs elimination of the catalysts reported in the literature.

Br-VOCs	Catalyst	SV (mL/(g · h))	Concentration (ppm)	$T_{90\%}$ (°C)	Ref.
DBM	RuB_1/TiO_2	60,000	500	182	[10]
DBM	Co_3O_4-K	112,500	500	271	[100]
DBM	Co_3O_4/CeO_2-rod	75,000	500	312	[101]
DBM	Co_4Ti_1	100,000	500	245	[102]
DBM	$RuSn/TiO_2$	120,000	500	>300	[103]
DBM	$Mn\text{-}Co/TiO_2$	75,000	500	325	[104]
DBM	$Co_3O_4/CeO_2\text{-}Co_3O_4$	112,500	500	321	[105]
DBM	Co–Mn–Ti	112,500	500	234	[106]
MB	Ru/TiO_2	60,000	100	212	[25]
MB	Ru/TiO_2	120,000	800	300	[26]
MB	$Ru/a\text{-}TiO_{2\text{-}180h}$	120,000	800	257	[27]
MB	$Ru/TiO_{2\text{-}700\text{-}4}$	120,000	800	<260	[107]
MB	$1\%Pt/30\%CeO_2\text{-}Al_2O_3$	90,000	34,000	<400	[108]

Low-temperature catalytic oxidation is of significant importance for the degradation of Br-VOCs, as it can avoid the formation of harmful byproducts with low energy consumption. Gao et al. [10] proposed a strategy for the modification of Ru/TiO_2 with boron. Compared to the limited electron transfer (0.02 e) in Ru/TiO_2, the Ru center acquired sufficient negative charge (0.31 e) through the strong p–d orbital hybridization (Figure 5a). The Ru–B site acted as an electron donor, complexing with the $2\pi^*$ antibonding orbitals of O_2, which alleviated the insufficiency of electron density in the metal center and achieved the activation of O_2, enabling the degradation of DBM at 182 °C. Liu et al. [25] worked on the oxidation of MB over the Ru catalysts loaded on various supports (e.g., TiO_2, SiO_2, Al_2O_3, and ZrO_2). The results revealed that the Ru particles tended to be anchored on the surface of rutile TiO_2. The Ru/TiO_2 material exhibited the highest catalytic activity ($T_{90\%}$ = 212 °C) for MB removal. Catalytic performance was affected by the nature of the support and the chemical state and dispersion of Ru. The main bromine-containing products of MB oxidation are HBr and Br_2, with no organic brominated byproducts being formed over the catalyst and the Br_2 selectivity being as high as 95%, which was originated from the direct oxidation of CH_3Br and the Deacon-like reaction of HBr. Additionally, the Ru/TiO_2 catalyst possessed good stability and Br resistance. Given the presence of substantial amounts of other pollutants in typical emissions containing MB (such as, carbon monoxide, aromatics, and methyl acetate), the authors [25] further explored the application of Ru/TiO_2 in catalytic oxidation under complex conditions. The results indicated that the Ru/TiO_2 catalyst could achieve simultaneous complete oxidation of these pollutants at 260 °C when MB (100 ppm), CO (3500 ppm), benzene (200 ppm), and methyl acetate (500 ppm) were co-present. Lv et al. [27] investigated the catalytic oxidation of MB over the Ru supported on titanium dioxide with different crystal phases. The Ru/anatase TiO_2 ($Ru/a\text{-}TiO_2$) catalyst demonstrated good stability after operation at 240 °C for 180 h. It was noted that within the initial 60 h of reaction, $Ru/a\text{-}TiO_2$ exhibited an induction activation, with the enhanced catalyst performance being closely related to the surface acidity (particularly medium-strength Lewis acidity). Although the size of Ru particles increased and the content of Ru^0 decreased as the reaction progressed, the formation of the RuO_xBr_y key species promoted an increase in both amount and strength of the acid sites in the catalyst. Additionally, when loading transition metals, the difference in valence between the dopant cations and the host cations could give rise to changes in catalytic performance. When Nb^{5+} was doped, TiO_2 acquired more sites with deficit electrons, thereby increasing the acidity. In contrast, the trend was reversed when other lower-valent transition metals (Ce, Co, Mn, and Ni) were added [27]. Furthermore, supported noble metal catalysts face several difficulties, such as high Ru loading, poor high-temperature resistance, and poor resistance to poisoning (easily deactivated by halogenated products like HBr and Br_2, which lead to deactivation and formation of the polybrominated byproducts). Notably, transition metal catalysts typically can effectively overcome the drawbacks of noble metal catalysts, especially their resistance to bromine poisoning, and thus have gained a considerable attention in catalytic Br-VOCs elimination in recent years. Mei et al. [100] prepared the different ordered mesoporous spinel-type Co_3O_4 catalyst using a hard-templating method, and compared it with the Co_3O_4 catalyst derived from the traditional precipitation route for CH_2Br_2 removal. The results demonstrated that the hard-templating-derived Co_3O_4 catalyst with an ordered mesoporous structure, a large surface area, a high Co^{3+} content, and a good redox ability exhibited better catalytic performance for CH_2Br_2 elimination. Meanwhile, the Co_3O_4 spinel-type catalyst also demonstrated a high CO_2 selectivity, a good stability, and no formation of the brominated organic byproducts. CeO_2 serves as a support that promotes the dispersion of metal oxides. By controlling the morphology (rod, plate or cube) of Co_3O_4/CeO_2, the interaction between the metal and the

support could be enhanced. Compared to the Co_3O_4/CeO_2-plate and Co_3O_4/CeO_2-cube catalysts, the Co_3O_4/CeO_2-rod catalyst exhibited a higher Co^{3+} concentration and an higher adsorbed oxygen content, with more oxygen vacancies being exposed on the (100) and (110) facets. The $T_{90\%}$ for the oxidation of DBM was 312 °C [101]. Mei et al. [102] introduced Ti into the Co_3O_4 crystal structure via the co-precipitation route, forming a Co–O–Ti solid solution. The Co_4Ti_1 (Co/Ti molar ratio = 4) exhibited a $T_{90\%}$ of 245 °C for the oxidation of DBM. The authors further simulated the catalytic oxidation of DBM in the presence of water vapor or p-xylene (PX) under actual operating conditions. The introduction of H_2O/PX led to a slight decrease in catalytic activity due to the competitive adsorption of CH_2Br_2 and H_2O/PX on the catalyst surface. Stability tests confirmed that Co_4Ti_1 maintained catalytic DBM elimination activity for at least 30 h of reaction in the presence of 2 vol% H_2O or 500 ppm PX. Furthermore, many VOCs purification companies have developed and applied catalysts for the combustion of Br-VOCs. For example, Topsoe's granular CK-302PTA catalyst (in which copper and manganese are used as the main active components) exhibits good high-temperature resistance and anti-poisoning ability, and is widely utilized in the treatment of PTA exhaust.

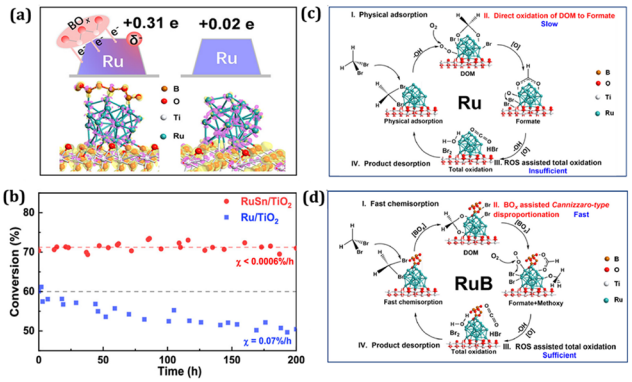

Figure 5. (**a**) Bader charge analysis of Ru/TiO_2 and RuB/TiO_2 [10]. Copyright 2023, American Chemical Society. (**b**) Long-term stability test of the $RuSn/TiO_2$ and Ru/TiO_2 catalysts [103]. Copyright 2025, American Chemical Society. (**c**,**d**) Scheme of DBM oxidation pathway/mechanism over Ru/TiO_2 and RuB/TiO_2 [10]. Copyright 2023, American Chemical Society.

Typical halogen poisoning of catalysts is triggered by the strong binding of halogens to metal centers, which leads to the occupation of active sites. Therefore, reducing the binding strength between halogens and metal centers to achieve rapid dehalogenation is a key approach to enhance resistance to halogen poisoning. Generally speaking, it is effective to employ conventional strategies (e.g., introducing Brønsted acid sites as dehalogenation centers) to improve the halogen tolerance of Ru-based catalysts [1,2]. Compared to chlorine, however, bromine poisoning may follow significantly different pathways. During Br-VOCs oxidation, surface bromine species can cause lattice oxygen displacement and severe lattice structure damage. Gao et al. [103] reported a Sn-mediated Ru–O covalent modulation strategy to stabilize the lattice oxygen of RuO_2 to prevent bromine poisoning. The optimized $RuSn_{0.25}/TiO_2$ catalyst demonstrated excellent stability within >200 h of DBM oxidation (Figure 5b). The results indicated that the electron redistribution of Ru caused by Sn doping and the downward shift of the O 2*p* band effectively passivated the lattice oxygen, protecting it from bromination. Lv et al. [107] investigated the stability of Ru/TiO_2 catalysts in the oxidation of MB, observing a gradual decline in catalytic activity as the reaction progressed that was attributable to the growth of Ru particles and the reduction of Ru^0 content. Ru particles were initially present as 2 nm and then aggregated into larger particles (5.4 nm). Concurrently, Ru^0 was progressively oxidized to the higher valence states. The addition of Ce could inhibit the oxidation of metallic Ru^0 by promoting electron transfer from the support to Ru and suppress Ru particles aggregation by increasing the oxygen electron density.

Figure 5c illustrates the oxidation process of DBM over Ru/TiO_2 [10]. The dioxymethylene (DOM) intermediate species originate from the dehalogenation reaction triggered by the reactive oxygen species (OH, O_2^{2-}, O_2^-, etc.), indicating that some DBM molecules underwent electrophilic substitutions with the surface oxygen species. DOM was directly oxidized to formate by the surface oxygen species, which further was oxidized to CO_x. Figure 5d depicts the oxidation process of DBM over RuB/TiO_2 [10]. The B sites as the Lewis acids readily dissociated DBM and DOM, with the DOM being rapidly converted to the formate species via a Cannizzaro-type reaction. Subsequently, formate was completely oxidized to CO_2 due to the enhanced oxidizing ability of RuB/TiO_2. The rapid step of DOM to formate catalyzed by the Lewis acid and the strong oxidizing ability endow RuB/TiO_2 to show a significantly higher low-temperature activity than Ru/TiO_2. Mei et al. [101] investigated the catalytic pathway of DBM oxidation over the Co_3O_4/CeO_2 catalyst and proposed similar viewpoints. Initially, the Br atoms in DBM are adsorbed at oxygen vacancies of Co_3O_4/CeO_2 and dissociated by the adjacent electrophilic oxygen species to form the bidentate methoxy species. Concurrently, they undergo the Cannizzaro-type disproportionation to generate the formate and methoxy species, which are then oxidized to CO_x by the active oxygen species derived from the dissociative adsorption of O_2 (Figure 6a). Lv et al. [26] utilized the HSAB (Hard–Soft-Acid–Base) theory to elucidate the differences in the dissociation of the C–Cl bonds in DCM and the C–Br bonds in MB. The HSAB theory categorizes acids and bases into three types based on their properties, namely hard, borderline, and soft ones.

 https://doi.org/10.53941/ges.2025.100012

The core principle of this theory is that hard acids tend to combine with hard bases. For the same catalyst, adsorption and competitive reactions strongly depend on the relative acid-base strength between the reactants and the catalyst. Therefore, the Cl atoms in DCM as the hard base are more readily bonded with the strong acid Ti^{4+}, whereas the Br atoms in MB serves as the borderline base (the Lewis base that lies between the hard and soft bases), preferentially complexing with the soft acid Ru^{2+}/Ru (Figure 6b).

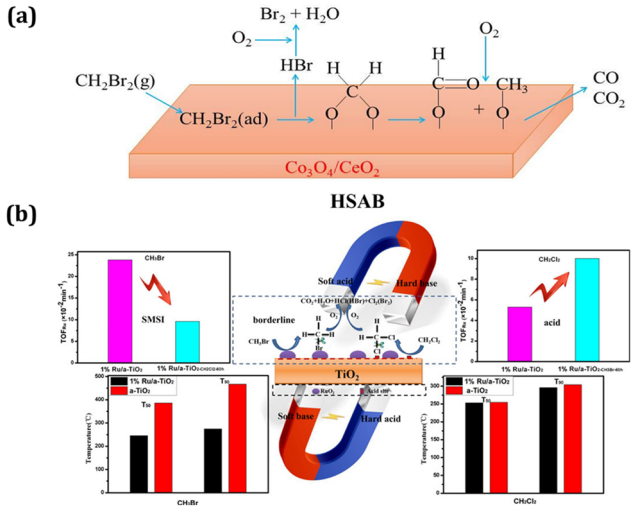

Figure 6. (**a**) A credible reaction mechanism for CH_2Br_2 oxidation over Co_3O_4/CeO_2. [101]. Copyright 2017, Elsevier. (**b**) The catalytic combustion performance of CH_2Br_2 and DCM over Ru/a-TiO_2 and its HSAB theory [26]. Copyright 2020, American Chemical Society.

4. Conclusions and Perspectives

The elimination of HVOCs is more complex than that of non-halogenated VOCs owing to the presence of the C–X (X = F, Cl or Br) bond. This review focuses on the typical HVOCs and analyzes their conformational relationships and reaction mechanisms throughout the catalytic lifecycle from the perspectives of catalyst preparation, catalytic reaction systems, and catalyst poisoning and deactivation. The first step in the catalytic oxidation of Cl-VOCs typically involves the adsorption at the hydroxyl or acidic sites on the catalyst, followed by the C–Cl bond cleavage, with the Cl being adsorbed on the catalyst and HCl being formed in the presence of surface –OH groups or dissociative H atoms. The resulting intermediates are further reacted with the active oxygen species to ultimately produce CO_2 and HCl. Dissociative Cl species adsorbed on the catalyst and HCl species formed on the catalyst that is not promptly removed will continue to react with the intermediates to produce more complicated polychlorinated byproducts than the original pollutants HVOCs. Catalytic performance and stability represent the most significant challenge faced by the catalytic HVOCs elimination technologies. The primary reasons for catalyst deactivation are generally inorganic halide adsorption and metal halide formation as well as carbon deposition. The adsorption of inorganic halides on the catalyst reduces the number of the active sites in catalyst, thereby undermining its catalytic performance. Water can act as a proton donor in the reaction, not only enhancing catalyst stability but also potentially facilitating the C–F bond activation more effectively than the surface –OH groups. Owing to the generation of highly corrosive, oxidative, and reactive HF or even F_2 in the decomposition of fluorinated organic compounds, higher demands are placed on chemical stability and corrosion resistance of the catalytic system, posing greater challenges in practical applications. The high selectivity towards Br_2 during the catalytic Br-VOCs combustion processes may give rise to rapid catalyst deactivation and generation of the polychlorinated byproducts. The currently developed catalysts for Br-VOCs elimination are often used for specific industries with more complex exhaust compositions under actual operating conditions. These characteristics pose new issues and challenges in developing the catalysts for the removal of brominated hydrocarbons. Ru-based catalysts exhibit high selectivities towards the final products (i.e., CO_2 and HCl). Transition metal oxides are extensively used owing to their low cost and strong resistance to poisoning. The selection of an appropriate support can induce a strong interaction between metal and support. Doping of transition metals can increase performance of the catalysts. The synergistic interaction of acidity and redox ability is crucial for ensuring the catalyst to perform well.

Although significant advancements have been made in catalytic elimination of the HVOCs in recent years, in which the various high-performance catalyst systems are developed, there are still many bottlenecks to be overcome to achieve large-scale industrial applications and to address the increasingly complex real-world environmental challenges. We believe that the future research should focus on the following key directions to drive the field towards deeper, broader, and smarter development:

(1) **Integrating advanced in situ characterization for precise analysis of catalyst structural dynamics and reaction mechanisms.** Future research should vigorously develop advanced in situ characterization techniques. In situ infrared/Raman spectroscopy and near-ambient pressure X-ray photoelectron spectroscopy can be employed to monitor the formation and transformation of reaction intermediates in real time. In situ X-ray absorption spectroscopy and environmental transmission electron microscopy can be utilized to observe the changes in the oxidation state and coordination environment of active metals, as well as the sintering or phase transformation of nanoparticles under

reaction conditions. This will clarify the deactivation mechanisms and provide guidance for regeneration strategies.

(2) **Focusing on complex real-world conditions to enhance catalyst practicality and tolerance**. Future catalytic research should explore the synergistic or inhibitory effects of multiple pollutants, high-concentration fluctuations, high humidity, SO_2, NO_x, dust, and other complex components on performance of the catalysts. Strengthening the assessment of catalyst regeneration behaviors and developing the efficient and low-energy regeneration processes are also essential.

(3) **Constructing AI-driven high-throughput platforms for intelligent catalyst development and optimization.** Future efforts should focus on constructing AI-based high-throughput computational and experimental platforms. Utilizing machine learning models to establish complex nonlinear mappings among catalyst composition, structure, preparation parameters, and catalytic performance can predict the potential excellent catalyst formulations.

(4) **Synergistic coupling of catalytic elimination with other technologies.** Traditional thermal catalytic technologies face challenges such as high energy consumption and susceptibility to poisoning when dealing with complex exhaust gases that are high in concentration and SV. Coupling catalysis with other forms of energy is an effective way to break through these bottlenecks, for example, synergistic photothermocatalysis, synergistic electrothermocatalysis, and plasma-assisted catalysis.

(5) **From harmlessness to valorization: developing high-value transformation technologies for HVOCs.** Future research should not be confined to the development of high-performance catalysts, but should be aimed to construct a comprehensive technological system that spans from fundamental research to resource recovery, for instance, functionalization of Cl-VOCs (e.g., converting CB and VC to phenols, chlorinated intermediates or non-halogenated aromatics), dehydrofluorination of HFCs (e.g., transforming 1,1-difluoroethane into vinyl fluoride), and halogen recovery (e.g., converting hydrogen halides into hydrochloric acid, hydrofluoric acid or other halogenated chemicals).

Author Contributions

Q.S.: writing—original draft editing, investigation; X.Y.: investigation; K.S.: investigation; L.W.: investigation; P.C.: investigation; Y.L.: methodology; J.D: methodology; Z.H.: visualization; H.D.: writing—reviewing and editing, conceptualization, methodology, supervision, project administration. All authors have read and agreed to the published version of the manuscript.

Funding

This work was financially supported by the National Natural Science Foundation of China (22322601, 22306008, and 22576008), R&D Program of Beijing Municipal Education Commission (KZ202210005011), Postdoctoral Science Foundation of China (2022M720315), Postdoctoral Research Foundation of Beijing (2023ZZ-139), and Science and Technology Plan Projects of the State Administration for Market Regulation (2021MK002).

Institutional Review Board Statement

Not applicable.

Informed Consent Statement

Not applicable.

Data Availability Statement

Not applicable.

Conflicts of Interest

The authors declare no conflict of interest.

Use of AI and AI-assisted Technologies

No AI tools were utilized for this paper.

References

1. He, C.; Cheng, J; Zhang, X.; et al. Recent advances in the catalytic oxidation of volatile organic compounds: A review based on pollutant sorts and sources. *Chem. Rev.* **2019**, *119*, 4471–4568.
2. Jia, H.; Xing, Y.; Zhang, L.; et al. Progress of catalytic oxidation of typical chlorined volatile organic compounds (CVOCs): A review. *Sci. Total Environ.* **2023**, *865*, 161063.
3. Han, W.; Kennedy, E.; Mackie, J.; et al. Conversion of a CFCs, HFCs and HCFCs waste mixture via reaction with methane. *J. Hazard. Mater.* **2010**, *184*, 696–703.
4. Yu, H.; Kennedy, E.; Adesinab, A.; et al. A review of CFC and halon treatment technologies—The nature and role of catalysts. *Catal. Surv. Asia* **2006**, *10*, 40–54.
5. Chen, Y.; Qu, W.; Luo, T.; et al. Promoting C–F bond activation via proton donor for CF_4 decomposition. *Proc. Natl. Acad. Sci. USA* **2024**, *120*, e2312480120.
6. Meng, X.; Dong, B.; Zhao, L.; et al. Synergistic regulation of charge state and electron-donating ability via heterojunctions design for fixation of electronegative greenhouse F-gases. *Appl. Catal. B* **2024**, *364*, 123709.
7. Paunović, V.; Pérez-Ramírez, J. Catalytic halogenation of methane: A dream reaction with practical scope? *Catal. Sci.*

Technol. **2019**, *9*, 4515–4530.
8. Paunović, V.; Hemberger, P.; Bodi, A.; et al. Evidence of radical chemistry in catalytic methane oxybromination. *Nat. Catal.* **2018**, *1*, 363–370.
9. He, J.; Xu, T.; Wang, Z.; et al. Transformation of methane to propylene: A two-step reaction route catalyzed by modified CeO_2 nanocrystals and zeolites. *Angew. Chem. Int. Ed.* **2012**, *51*, 2438–2442.
10. Gao, G.; Wei, L.; Liu, Z.; et al. Electron donation from boron suboxides via strong p–d orbital hybridization boosts molecular O_2 activation on Ru/TiO_2 for low-temperature dibromomethane oxidation. *Environ. Sci. Technol.* **2023**, *57*, 17566–17576.
11. Molina, M.J.; Rowland, F.S. Stratospheric sink for chlorofluoromethanes: Chlorine atom-catalysed destruction of ozone. *Nature* **1974**, *249*, 810–812.
12. Lin, H.; Liu, Y.; Deng, J.; et al. The advancement of supported bimetallic catalysts for the elimination of chlorinated volatile organic compounds. *Catalysts* **2024**, *14*, 531.
13. Sheraz, M.; Anus, A.; Le, V.C.T.; et al. A comprehensive review of contemporary strategies and approaches for the treatment of HFC-134a. *Greenh. Gases* **2021**, *11*, 1118–1133.
14. Takita, Y.; Tanabe, T.; Ito, M.; Decomposition of CH_2FCF_3 (134a) over metal phosphate catalysts. *Ind. Eng. Chem. Res.* **2002**, *41*, 2585–2590.
15. Ma, Z.; Hua, W.; Tang, Y; et al. Catalytic hydrolysis of CFC-12 over solid acid $Ti(SO_4)_2$. *Chin. Chem. Lett.* **2000**, *11*, 311–314.
16. Fu, X.; Zeltner, W.A.; Yang, Q; et al. Catalytic hydrolysis of dichlorodifluoromethane (CFC-12) on sol-gel-derived titania unmodified and modified with H_2SO_4. *J. Catal.* **1997**, *168*, 482–490.
17. Ma, Z.; Hua, W.; Tang, Y; et al. Catalytic decomposition of CFC-12 on solid acids SO_4^{2-}/M_xO_y (M = Zr, Ti, Sn, Fe, Al). *Chin. J. Chem.* **2000**, *18*, 241–245.
18. Ma, Z.; Hua, W.; Tang, Y.; et al. Catalytic decomposition of CFC-12 over solid acids WO_3/M_xO_y (M = Ti, Sn, Fe). *J. Mol. Catal. A* **2000**, *159*, 335–345.
19. Ding, S.; Wu, S.; Wang, P.; et al. Structure-selectivity relevance of multiple-component catalysts for CVOCs' complete oxidation: State-of-the-art and perspectives. *Sep. Purif. Technol.* **2025**, *354*, 128964.
20. Yu, X.; Dai, L.; Deng, J.; et al. Catalytic performance and intermediates identification of trichloroethylene deep oxidation over Ru/3DOM SnO_2 catalysts. *J. Catal.* **2021**, *400*, 310–324.
21. Yu, X.; Dai, L.; Peng, Y.; et al. High selectivity to HCl for the catalytic removal of 1,2-dichloroethane over RuP/3DOM WO_x: Insights into the effects of P-doping and H_2O introduction. *Environ. Sci. Technol.* **2021**, *55*, 14906–14916.
22. Wu, L.; Liu, Y.; Yu, X.; et al. Constructing bridge hydroxyl groups on the Ru/MO_x/HZSM-5 (M = W, Mo) catalysts to promote the hydrolysis oxidation of multicomponent VOCs. *Environ. Sci. Technol.* **2024**, *59*, 945–955.
23. Wu, L.; Deng, J.; Liu, Y.; et al. Enhanced removal efficiency of multicomponent VOCs over the Sn-doped silicalite-1-supported Ru Single-atom catalysts by constructing tightly coupled redox and acidic sites. *Appl. Catal. B* **2024**, *351*, 123910.
24. Yu, X.; Deng, J.; Liu, Y.; et al. Enhanced water resistance and catalytic performance of Ru/TiO_2 by regulating Brønsted acid and oxygen vacancy for the oxidative removal of 1,2-dichloroethane and toluene. *Environ. Sci. Technol.* **2022**, *56*, 11739–11749.
25. Liu, X.; Zeng, J.; Wang, J.; et al. Catalytic oxidation of methyl bromide using ruthenium-based catalysts. *Catal. Sci. Technol*. **2016**, *6*, 4337–4345.
26. Lv, L.; Wang, S.; Ding, Y.; et al. Reaction mechanism dominated by the Hard-Soft Acid-Base theory for the oxidation of CH_2Cl_2 and CH_3Br over a titanium oxide-supported Ru catalyst. *Ind. Eng. Chem. Res.* **2020**, *59*, 7383–7388.
27. Lv, L.; Wang, S.; Ding, Y.; et al. Mechanistic insights into the contribution of Lewis acidity to brominated VOCs combustion over titanium oxide supported Ru catalyst. *Chemosphere* **2021**, *263*, 128112.
28. Tian, R.; Lu, J.; Xu, Z.; et al. Unraveling the synergistic reaction and the deactivation mechanism for the catalytic degradation of double components of sulfur-containing VOCs over ZSM-5-based materials. *Environ. Sci. Technol.* **2023**, *57*, 1443–1455.
29. Wang, X.; Li, Z.; Gao, R.; et al. Photothermal catalytic removal of 1,2-DCE with high HCl selectivity over the Brønsted acid-enriched sulfur-doped MOFs. *Environ. Sci. Technol.* **2024**, *58*, 17190–17200.
30. Zhang, C.; Gao, F.; Luo, N.; et al. Recent advances of chlorobenzene catalytic oxidation: influencing factors, roles of active sites and optimization. *Sep. Purif. Technol.* **2025**, *376*, 133962.
31. Feng, Y.; Jiang, Y.; Hua, M.; et al. Cooking oil fumes: A comprehensive review of emission characteristics and catalytic oxidation strategies. *ACS EST Eng.* **2025**, *5*, 303–324.
32. Li, Z.; Gao, R.; Hou, Z.; et al. Tandem supported Pt and ZSM-5 catalyst with separated catalytic functions for promoting multicomponent VOCs oxidation. *Appl. Catal. B* **2023**, *339*, 123131.
33. Maupin, I.; Pinard, L.; Mijoin, J.; et al. Bifunctional mechanism of dichloromethane oxidation over Pt/Al_2O_3: CH_2Cl_2 disproportionation over alumina and oxidation over platinum. *J. Catal.* **2012**, *291*, 104–109.
34. Bahareh, A.T.; Eskandari, S.; Khan, U.; et al. A review of preparation methods for supported metal catalysts. *Adv. Catal.* **2017**, *61*, 1–35.
35. Munnik, P.; De Jongh, P.E.; De Jong, K.P. Recent developments in the synthesis of supported catalysts. *Chem. Rev.* **2015**, *115*, 6687–6718.
36. Zhang, Y.; Zhang, G.; Liu, J.; et al. Insight into the role of preparation method on the structure and size effect of Ni/MSS catalysts for dry reforming of methane. *Fuel Process. Technol.* **2023**, *250*, 107891.

37. Wang, J.; Liu, X.; Zeng, J.; et al. Catalytic oxidation of trichloroethylene over TiO_2 supported ruthenium catalysts. *Catal. Commun.* **2016**, *76*,13–18.
38. Deraz, N.M. The comparative jurisprudence of catalysts preparation methods: II. Deposition-precipitation and adsorption methods. *J. Ind. Environ. Chem.* **2018**, *2*, 1–3.
39. Wang, T.; Liu, S.; Wang, L.; et al. High-performance Rh/CeO_2 catalysts prepared by L-lysine-assisted deposition precipitation method for steam reforming of toluene. *Fuel* **2023**, *341*, 127736.
40. Simon, P.; Zanfoni, N.; Avril, L.; et al. Nanoporous platinum doped cerium oxides thin films grown on silicon substrates: Ionic platinum localization and stability. *Adv. Mater. Interfaces* **2017**, *4*, 1600821.
41. Hou, Z.; Lu, Y.; Liu, Y.; et al. A general dual-metal nanocrystal dissociation strategy to generate robust high-temperature-stable alumina-supported single-atom catalysts. *J. Am. Chem. Soc.* **2023**, *145*, 15869–15878.
42. Qiu, J.; Peng, Y.; Tang, M.; et al. Catalytic activity, selectivity, and stability of co-precipitation synthesized Mn-Ce mixed oxides for the oxidation of 1,2-dichlorobenzene. *Environ. Sci. Pollut. Res. Int.* **2021**, *28*, 65416–65427.
43. Wang, X.; Kang, Q.; Li, D. Catalytic combustion of chlorobenzene over MnO_x–CeO_2 mixed oxide catalysts. *Appl. Catal. B* **2009**, *86*, 166–175.
44. Feng, X.; Zheng, Y.; Lin, D.; et al. Novel synthetic route to Ce-Cu-W-O microspheres for efficient catalytic oxidation of vinyl chloride emissions. *Chin. J. Catal.* **2020**, *41*, 1864–1872.
45. Tian, M.; Jian, Y.; Ma, Y.; et al. Rational design of $CrO_x/LaSrMnCoO_6$ composite catalysts with superior chlorine tolerance and stability for 1,2-dichloroethane deep destruction. *Appl. Catal. A* **2019**, *570*, 62–72.
46. Liu, J.; Wang, Y.; Dai, Z.; et al. Recent advances in Zeolite-Based catalysts for volatile organic compounds decontamination by thermal catalytic oxidation. *Sep. Purif. Technol.* **2024**, *330*, 125339.
47. Wu, L.; Liu, Y.; Jia, Y.; et al. A novel strategy for enhancing resistance to chlorine, water, and sulfur oxide of the Pt/Co-ZSM-5 catalyst by synergistic coupling of acidity and redox sites for the oxidation of multicomponent VOCs. *Appl. Catal. B* **2025**, *378*, 125557.
48. Gołąbek, K.; Palomares, A.E.; Martínez-Triguero, J.; et al. Ce-modified zeolite BEA catalysts for the trichloroethylene oxidation. The role of the different and necessary active sites. *Appl. Catal. B* **2019**, *259*, 118022.
49. Sun, Q.; Yu, X.; Wu, L.; et al. Boosting catalytic and anti-fluorination performance of the Ru/vanadia–titania catalyst for the oxidative destruction of Freon by sulfuric acid modification. *Environ. Sci. Technol.* **2024**, *58*, 12719–12730.
50. Karmakar, S.; Greene, H.L. An investigation of CFC12 (CCl_2F_2) decomposition on TiO_2 catalyst. *J. Catal.* **1995**, *151*, 394–406.
51. Li, Y.; Ren, Y.; Xiao, H.; et al. Recent advances of the effect of H_2O on VOC oxidation over catalysts: Influencing factors, inhibition/promotion mechanisms, and water resistance strategies. *Environ. Sci. Technol.* **2025**, *59*, 1034–1059.
52. Zhang, H.; Luo, T.; Long, Y.; et al. Identification of the active site during CF_4 hydrolytic decomposition over γ-Al_2O_3. *Environ. Sci. Nano* **2022**, *9*, 954–963.
53. Takita, Y.; Morita, C.; Ninomiya, M.; et al. Catalytic decomposition of CF_4 over $AlPO_4$-based catalyst. *Chem. Lett.* **1999**, 417–418.
54. Zhang, H.; Liu, K.; Chen, Y.; et al. Efficient and stable CF_4 decomposition over θ-Al_2O_3 with extraordinary resistance to HF. *Environ. Sci. Nano* **2023**, *10*, 3149–3155.
55. Luo, T.; Chen, Y.; Liu, K.; et al. Rational design of active sites in alumina-based catalysts to optimize antibonding-orbital occupancy for tetrafluoromethane decomposition. *Environ. Sci. Nano* **2023**, *10*, 3307–3316.
56. Xu, X.; Jeon, J.Y.; Choi, M.H.; et al. The modification and stability of γ-Al_2O_3 based catalysts for hydrolytic decomposition of CF_4. *J. Mol. Catal. A.* **2007**, *266*, 131–138.
57. Jeon, H.; Oh, M.; Han, J.W.; et al. Understanding remarkable promotional effects of Zn on alumina in catalytic hydrolysis of perfluorocarbon. *J. Catal.* **2023**, *426*, 361–367.
58. Li, Z.; Tan, X.; Ren, G.; et al. Equivalence of difluorodichloromethane (CFC-12) hydrolysis catalyzed by solid acid (base) MoO_3(MgO)/ZrO_2. *RSC Adv.* **2020**, *10*, 33662–33674.
59. Takita, Y.; Wakamatsu, H.; Tokumaru, M.; et al. Decomposition of chlorofluorocarbons over metal phosphate catalysts III.: Reaction path of CCl_2F_2 decomposition over $AlPO_4$. *Appl. Catal. A* **2000**, *194*, 55–61.
60. Ning, P.; Wang, X.; Bart, H.; et al. Catalytic decomposition of CFC-12 over solid superacid Mo_2O_3/ZrO_2. *J. Environ. Eng.* **2011**, *137*, 897–902.
61. Han, T.U.; Yoo, B.S.; Kim, Y.M.; et al. Catalytic conversion of 1,1,1,2-tetrafluoroethane (HFC-134a). *Korean J. Chem. Eng.* **2018**, *35*, 1611–1619.
62. Swamidoss, C.M.A.; Sheraz, M.; Anus, A.; et al. Effect of Mg/Al_2O_3 and calcination temperature on the catalytic decomposition of HFC-134a. *Catalysts* **2019**, *9*, 270.
63. Kim, M.J.; Kim, Y.; Youn, J.R.; et al. Effects of sulfuric acid treatment on the performance of Ga-Al_2O_3 for the hydrolytic decomposition of 1,1,1,2-tetrafluoroethane (HFC-134a). *Catalysts* **2020**, *10*, 766.
64. El-Bahy, Z.; Ohnishi, R.; Ichikawa, M. Hydrolysis of CF_4 over alumina-based binary metal oxide catalysts. *Appl. Catal. B* **2003**, *40*, 81–91.
65. Digne, M.; Sautet, P.; Raybaud, P.; et al. Hydroxyl groups on γ-alumina surfaces: A DFT study. *J. Catal.* **2002**, *211*, 1–5.
66. Nortier, P.; Fourre, P.; Mohammed Saad, A.B.; et al. Effects of crystallinity and morphology on the surface properties of alumina. *Appl. Catal.* **1990**, *61*, 141–160.
67. Murrayrust, P.; Stallings, W.; Monti, C.; et al. Intermolecular interactions of the C–F bond: The crystallographic environment of fluorinated carboxylic acids and related structures. *J. Am. Chem. Soc.* **1983**, *105*, 3206–3214.
68. Cormanich, R.A.; Rittner, R.; Freitas, M.P.; et al. The seeming lack of CF…HO intramolecular hydrogen bonds in

linear aliphatic fluoroalcohols in solution. *Phys. Chem. Chem. Phys.* **2014**, *16*, 19212–19217.
69. Luo, T.; Zhang, H.; Chen, Y.; et al. Unveiling tetrafluoromethane decomposition over alumina catalysts. *J. Am. Chem. Soc.* **2024**, *146*, 35057–35063.
70. Wang, X.; Fu, J.; Zhang, H.; et al. Detoxification of carbonaceous species for efficient perfluorocarbon hydrolysis. *Environ. Sci. Technol.* **2025**, *59*, 3309–3315.
71. Takita, Y.; Moriyama, J.; Yoshinaga, Y.; et al. Adsorption of water vapor on the $AlPO_4$-based catalysts and reaction mechanism for CFCs decomposition. *Appl. Catal. A* **2004**, *271*, 55–60.
72. Ng, C.F.; Shan, S.; Lai, S. Catalytic decomposition of CFC-12 on transition metal chloride promoted γ-alumina. *Appl. Catal. B* **1998**, *16*, 209–217.
73. Gong-Liang, L.; Hiroyasu, N.; Tatsumi, I.; et al. Catalytic dehydrouorination of CF_3CH_3(HFC143a) into CF_2CH_2(HFC1132a). *Appl. Catal. B* **1998**, *16*, 309–317.
74. Tu, C.; Zhang, H.; Wang, X.; et al. Phase-Engineered ZrO_2 for tuning catalytic oxidation of dichloromethane over W/ZrO_2: Zr-doped WO_x clusters and the hydrolysis-oxidation mechanism. *Environ. Sci. Technol.* **2025**, *58*, 2838–2848.
75. Wang, W.; Zhu, Q.; Dai, Q.; et al. Fe doped CeO_2 nanosheets for catalytic oxidation of 1,2-dichloroethane: Effect of preparation method. *Chem. Eng. J.* **2017,** *307*, 1037–1046.
76. Zhang, X.; Dai, L.; Liu, Y.; et al. Effect of support nature on catalytic activity of the bimetallic RuCo nanoparticles for the oxidative removal of 1,2-dichloroethane. *Appl. Catal. B* **2021**, *285*, 119804.
77. Tian, M.; Guo, X.; Dong, R.; et al. Insight into the boosted catalytic performance and chlorine resistance of nanosphere-like meso-macroporous CrO_x/$MnCo_3O_x$ for 1,2-dichloroethane destruction. *Appl. Catal. B* **2019**, *259*, 118018.
78. Cao, S.; Wang, H.; Yu, F.; et al. Catalyst performance and mechanism of catalytic combustion of dichloromethane (CH_2Cl_2) over Ce doped TiO_2. *J. Colloid Interface Sci.* **2016,** *463*, 233–241.
79. Dai, Q.; Zhang, Z.; Yan, J.; et al. Phosphate-functionalized CeO_2 nanosheets for efficient catalytic oxidation of dichloromethane. *Environ. Sci. Technol.* **2018**, *52*, 13430–13437.
80. Zhang, X.; Liu, Y.; Deng, J.; et al. Alloying of gold with palladium: An effective strategy to improve catalytic stability and chlorine-tolerance of the 3DOM CeO_2-supported catalysts in trichloroethylene combustion. *Appl. Catal. B* **2019**, *257*, 117879.
81. Gao, R.; Zhang, M.; Liu, Y.; et al. Engineering platinum catalysts via a site-isolation strategy with enhanced chlorine resistance for the elimination of multicomponent VOCs. *Environ. Sci. Technol.* **2022**, *56*, 9672–9682.
82. Zhang, X.; Liu, Y.; Deng, J.; et al. Three-dimensionally ordered macroporous Cr_2O_3–CeO_2: High-performance catalysts for the oxidative removal of trichloroethylene. *Catal. Today* **2020**, *339*, 200–209.
83. Scirè, S.; Minicò, S.; Crisafulli, C. Pt catalysts supported on H-type zeolites for the catalytic combustion of chlorobenzene. *Appl. Catal. B* **2003**, *45*, 117–125.
84. He, C.; Yu, Y.; Shi, J.; et al. Mesostructured Cu–Mn–Ce–O composites with homogeneous bulk composition for chlorobenzene removal: Catalytic performance and microactivation course. *Mater. Chem. Phys.* **2015**, *157*, 87–100.
85. Gu, Y.; Cai, T.; Gao, X.; et al. Catalytic combustion of chlorinated aromatics over WO_x/CeO_2 catalysts at low temperature. *Appl. Catal. B* **2019**, *248*, 264–276.
86. Deng, Y.; Shang, Y.; Huang, T.; et al. Reversing the HCl/Cl_2 selectivity for efficient catalytic elimination of dichloromethane by incorporation of Ti^{4+} into CeO_2 lattice. *Appl. Catal. B* **2025**, *373*, 125338.
87. Van den Brink, R.W.; Mulder, P.; Louw, R.; et al. Catalytic oxidation of dichloromethane on γ-Al_2O_3: A combined flow and infrared spectroscopic study. *J. Catal.* **1998**, *180*, 153–160.
88. Yang, Y.; Liu, S.; Zhao, H.; et al. Promotional effect of doping Cu into cerium-titanium binary oxides catalyst for deep oxidation of gaseous dichloromethane. *Chemosphere* **2019**, *214*, 553–562.
89. Yin, L.; Lu, G.; Gong, X. A DFT+U study of the catalytic degradation of 1,2-dichloroethane over CeO_2. *Phys. Chem. Chem. Phys.* **2018**, *20*, 5856–5864.
90. Fei, Z.; Cheng, C.; Chen, H.; et al. Construction of uniform nanodots CeO_2 stabilized by porous silica matrix for 1,2-dichloroethane catalytic combustion. *Chem. Eng. J.* **2019**, *370*, 916–924.
91. Yang, P.; Xue, X.; Meng, Z.; et al. Enhanced catalytic activity and stability of Ce doping on Cr supported HZSM-5 catalysts for deep oxidation of chlorinated volatile organic compounds. *Chem. Eng. J.* **2013,** *234*, 203–210.
92. Lin, F.; Xiang, L.; Zhang, Z.; et al. Comprehensive review on catalytic degradation of Cl-VOCs under the practical application conditions. *Crit. Rev. Environ. Sci. Technol.* **2020**, *52*, 311–355.
93. Wang, L.; Wang, C.; Xie, H.; et al. Catalytic combustion of vinyl chloride over Sr doped $LaMnO_3$. *Catal. Today* **2019**, *327*, 190–195.
94. Zhang, C.; Wang, C.; Zhan, W.; et al. Catalytic oxidation of vinyl chloride emission over $LaMnO_3$ and $LaB_{0.2}Mn_{0.8}O_3$ (B = Co, Ni, Fe) catalysts. *Appl. Catal. B* **2013**, *129*, 509–516.
95. Huang, H.; Dai, Q.; Wang, X. Morphology effect of Ru/CeO_2 catalysts for the catalytic combustion of chlorobenzene. *Appl. Catal. B* **2014**, *158–159*, 96–105.
96. Van Den Brink, R.W.; Louw, R.; Mulder, P. Formation of polychlorinated benzenes during the catalytic combustion of chlorobenzene using a Pt/γ-Al_20_3 catalyst. *Appl. Catal. B* **1998**, *16*, 219–226.
97. Sun, P.; Wang, W.; Dai, X.; et al. Mechanism study on catalytic oxidation of chlorobenzene over $Mn_xCe_{1-x}O_2$/H-ZSM5 catalysts under dry and humid conditions. *Appl. Catal. B* **2016,** *198*, 389–397.
98. Gao, F.; Chen, D.; Luo, N.; et al. Catalytic performance and

reaction mechanism of chlorobenzene oxidation over MnO_x-CeO_2 catalyst. *Chem. J. Chin. Univ.* **2023**, *44*, 20220690.

99. Long, G.; Chen, M.; Li, Y.; et al. One-pot synthesis of monolithic Mn-Ce-Zr ternary mixed oxides catalyst for the catalytic combustion of chlorobenzene. *Chem. Eng. J.* **2018**, *360*, 964–973.
100. Mei, J.; Xie, J.; Qu, Z.; et al. Ordered mesoporous spinel Co_3O_4 as a promising catalyst for the catalytic oxidation of dibromomethane. *Mol. Catal*. **2018**, *461*, 60–66.
101. Mei, J.; Ke, Y.; Yu, Z.; et al. Morphology-dependent properties of Co_3O_4/CeO_2 catalysts for low temperature dibromomethane (CH_2Br_2) oxidation. *Chem. Eng. J*. **2017**, *320*, 124–134.
102. Mei, J.; Huang, W.; Qu, Z.; et al. Catalytic oxidation of dibromomethane over Ti-modified Co_3O_4 catalysts: Structure, activity and mechanism. *J. Colloid Interface Sci.* **2017**, *505*, 870–883.
103. Gao, G.; Hou, J.; Fan, Y.; et al. Stabilizing Ru-Based catalysts against bromine poisoning through Ru–O Covalency regulation for durable brominated volatile organic compound oxidation. *Environ. Sci. Technol.* **2025**, *59*, 15504–15514.
104. Mei, J.; Zhao, S.; Huang, W.; et al. Mn-Promoted Co_3O_4/TiO_2 as an efficient catalyst for catalytic oxidation of dibromomethane (CH_2Br_2). *J. Hazard. Mater.* **2016**, *318*, 1–8.
105. Mei, J.; Xie, J.; Sun, Y.; et al. Design of Co_3O_4/CeO_2–Co_3O_4 hierarchical binary oxides for the catalytic oxidation of dibromomethane. *J. Ind. Eng. Chem.* **2019**, *73*, 134–141.
106. Mei, J.; Qu, Z.; Zhao, S.; et al. Promoting effect of Mn and Ti on the structure and performance of Co_3O_4 catalysts for oxidation of dibromomethane. *J. Ind. Eng. Chem.* **2017**, *57*, 208–215.
107. Lv, L.; Wang, S.; Ding, Y.; et al. Deactivation mechanism and anti-deactivation modification of Ru/TiO_2 catalysts for CH_3Br oxidation. *Chemosphere* **2020**, *257*, 127249.
108. Chen, C.Y.; Pignatello, J.J. Catalytic oxidation for elimination of methyl bromide fumigation emissions using ceria-based catalysts. *Appl. Catal. B* **2013,** *142–143*, 785–794.